



Highlights from the RICH 2022 Conference

Antonis Papanestis
STFC/RAL

RICH = Ring Imaging Cherenkov detector

Edinburgh Sep 2022



Looking back as well as forward



The RICH Revolution

1979 \Rightarrow 1981

Benzene \rightarrow TEA \rightarrow THAE

LIF \rightarrow CaF₂ \rightarrow Quartz

Cryogenic noble liquids \rightarrow Warm CaF₂ liquids

MWPC \rightarrow TPC

Spherical liquid RICH \rightarrow Cylindrical liquid RICH

Spherical gaseous RICH \rightarrow Cylindrical gaseous RICH

Outside B-field \rightarrow Inside B-field

Separate gas & liq. detector \rightarrow Integrated gas & liq. det.

\Rightarrow DELPHI RICH

\approx CRID \approx UA2 RICH \approx ...

NUCLEAR INSTRUMENTS AND METHODS 141 (1977) 371-381 © NORTH-HOLLAND PUBLISHING CO.

PHOTO-IONIZATION AND CHERENKOV RING IMAGING

J. SEGUINOT and J. VITALENTI*

CHERENKOV RING DETECTOR

Received 11 December 1976

We have investigated the photo-ionization process in gases and show that simple photon polar counting in multichannel proportional chambers (MPCs) is possible with about 50% overall efficiency for photons above 3.7 eV. An application of this technique to imaging the Cherenkov sub-nanosecond (ns) radiation is presented.

1. Introduction

The Cherenkov radiation effect in an optical medium allows a precise determination of the velocity v (or $\beta = v/c$) of a charged particle passing through the medium. From the Cherenkov angle θ_c (1)

$$\cos \theta_c = 1/\beta n$$

where θ_c is the emission angle of the Cherenkov light and n the refractive index of the optical medium, we find

$$\beta = [n^2 \sin^2 \theta_c + 1]^{-1/2}$$

with $\Delta \theta_c$ and Δn as the r.m.s. error in the measurement of θ_c and n respectively. Liu and Mounier¹ show that with a "differential nuclear detector" (DND) type Cherenkov counter (DND) a resolution of $\Delta \beta/\beta = 0.1\%$ is possible. This corresponds to a β resolution of $\Delta \beta/\beta = 0.4\%$ at $\beta = 0.999$. In such conditions the Cherenkov photons emitted at different points along the particle's straight line trajectory form a ring of radius r in the focal plane. In the small angle approximation the focal surface is a plane and the radius of the ring image is

$$r = f \sin \theta_c$$

The single determination in DND is obtained by using an annular diaphragm of radius r at the mirror focal plane. Photomultiplier (PMT) located behind the diaphragm detect the transmitted photons. For optimal resolution additional optical elements are added to correct for chromatic distortions due to the variation of n with the energy of

the emitted photons. Obviously a DND type counter can only be used in reflected beams so that the source of Cherenkov radiation is along the optical axis of the device. Furthermore, the counter is not necessarily sensitive to β and responds only to particles having a given value of β (i.e. only to particles having a given velocity through the counter). Such counters are suitable for velocity transfer in collimated momentum analysis; particles velocity measurement of secondary particles emerging from an interaction. The phase space occupied by these particles is large whereas the counter acceptance of DND is small.

A secondary particle detector may be designed to measure the position of a spherical surface of radius R whose centre is the source of secondary particles (target) and a spherical detector surface of radius R with the Cherenkov radiating medium

Fig. 1. Schematic large phase space acceptance Cherenkov ring imaging detector.

* And CNRS (France), ¹ now at CERN, Saclay, France.

Homage to Jacques Seguinot

BTeV RICH

RICH 2022

- BTeV RICH prototype**
 - Built at Syracuse and tested with beams at Fermilab
 - Presented at RICH2004

June 2 - July 4, 2004

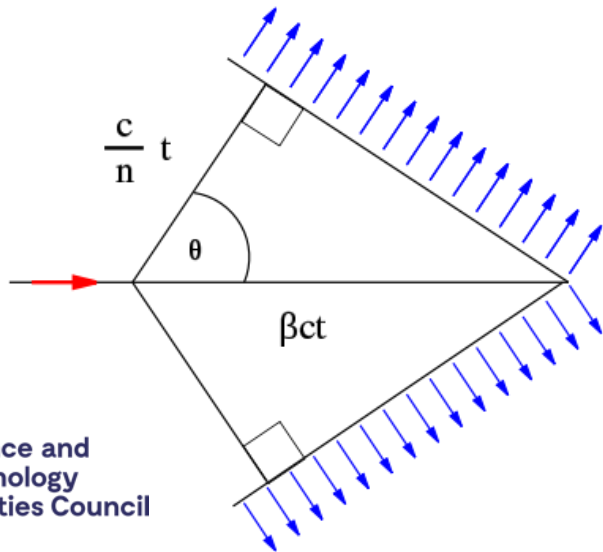
Ring produced by a single 120 GeV proton

12/09/2022 Franz Muheim - RICH2022 16

Homage to Sheldon Stone



Cherenkov radiation



Cherenkov principles



Threshold:

$$\beta_{th} = \frac{v_{th}}{c} = \frac{1}{n(\lambda)}$$

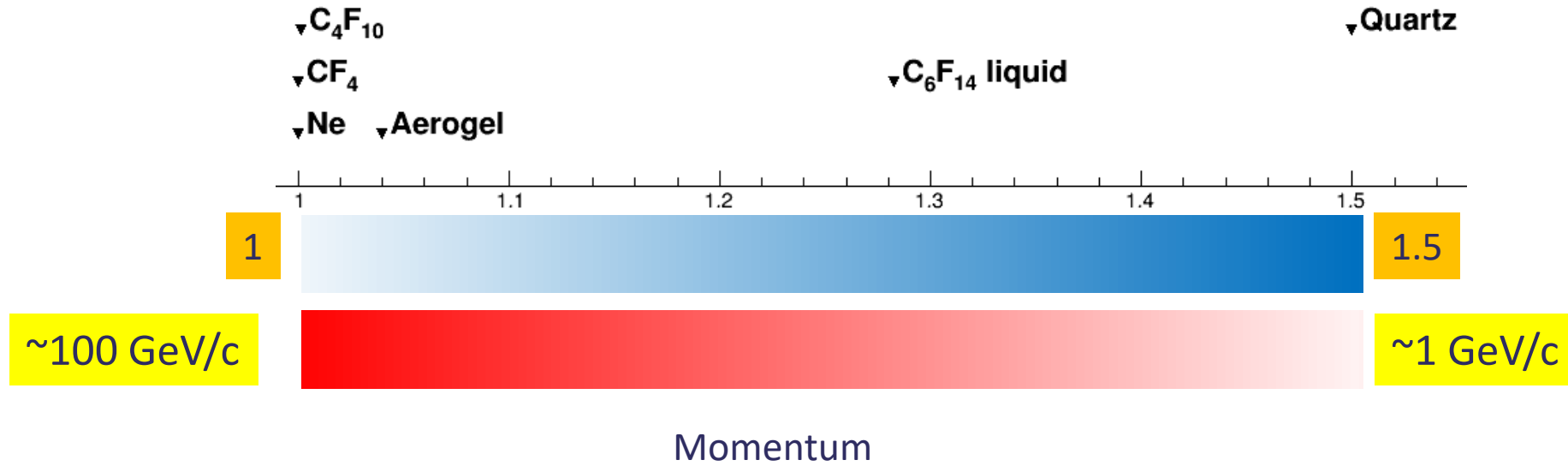
Cherenkov angle:

$$\cos \theta_c = \frac{1}{\beta n(\lambda)}$$

Number of produced photons:

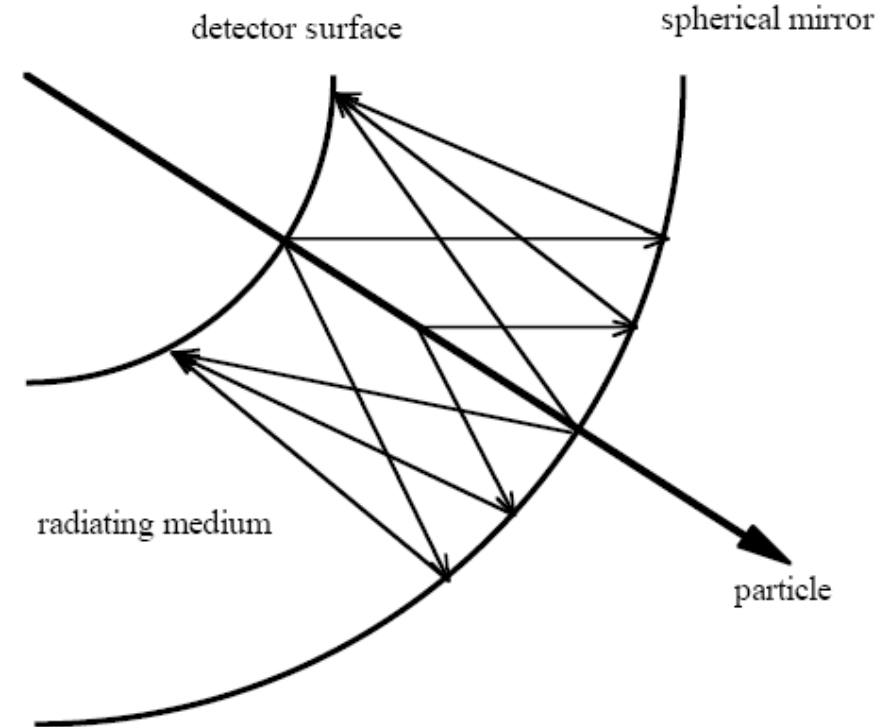
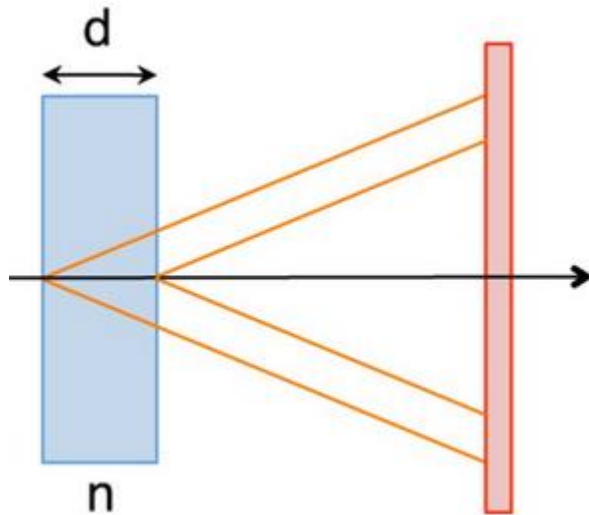
$$N_{photons} = L \frac{\alpha}{\hbar c} Z^2 \int \sin^2 \theta_c(E) dE$$

Refractive index range



RICH Detectors

Proximity focusing geometry



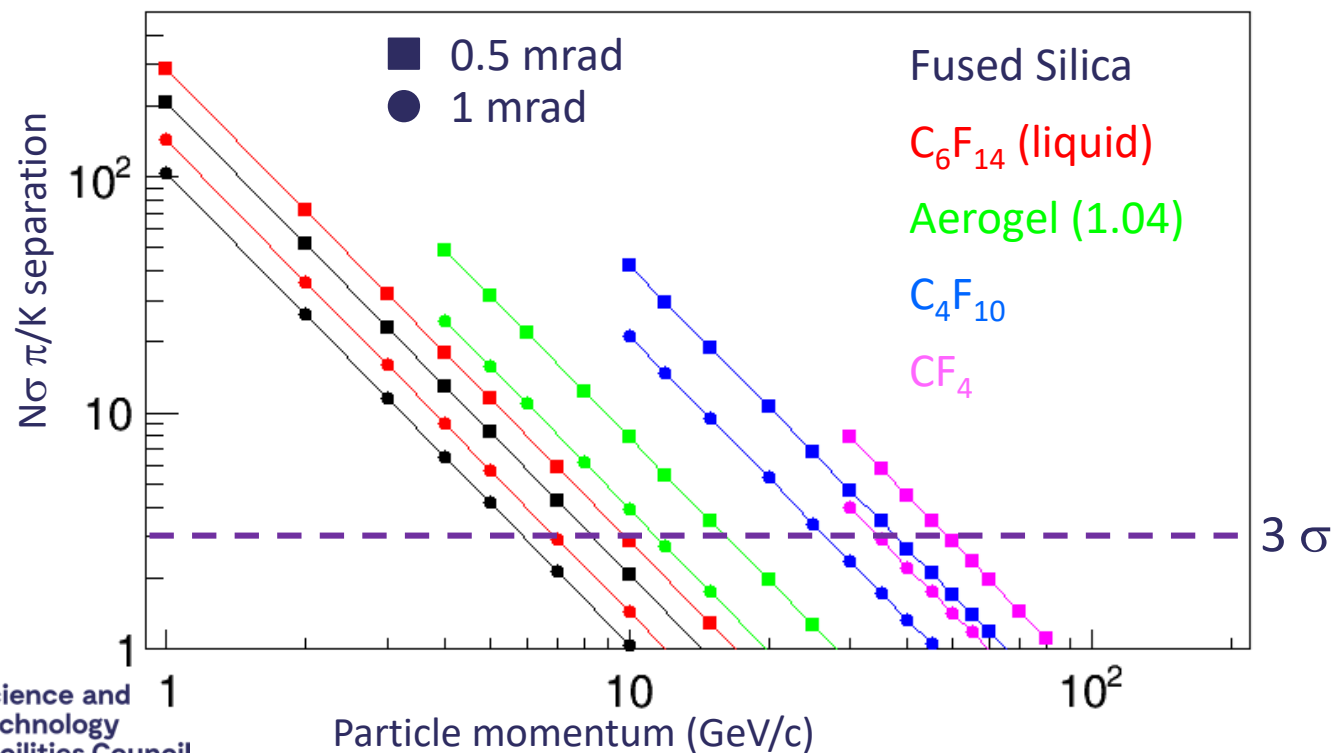
- Measures both the Cherenkov angle and the number of photoelectrons detected.
- Can be used over particle identification over large surfaces.
- Requires photodetectors with single photon identification capability.

RICH performance

$$N_\sigma \approx \frac{|m_1^2 - m_2^2|}{2P^2\sigma[\theta_c(tot)]\sqrt{n^2 - 1}}$$

For particles well above threshold

B. N. Ratcliff, NIMA 502 (2003) 211-221



$\sigma[\theta_c(tot)]$ components:

- Emission point error
- Detection point error (pixel size)
- Chromatic error



Science and
Technology
Facilities Council



The performance of the LHCb RICH detectors during the runs 1 and 2 of the LHC



Antonis Papanestis
STFC – RAL
on behalf of the LHCb RICH Collaboration

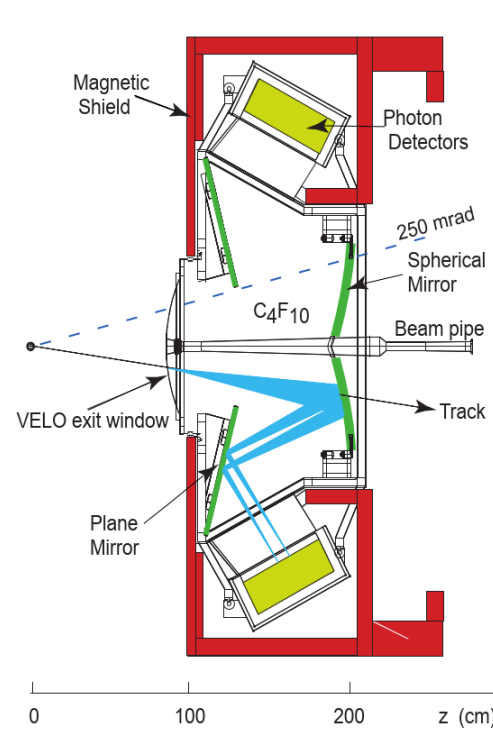
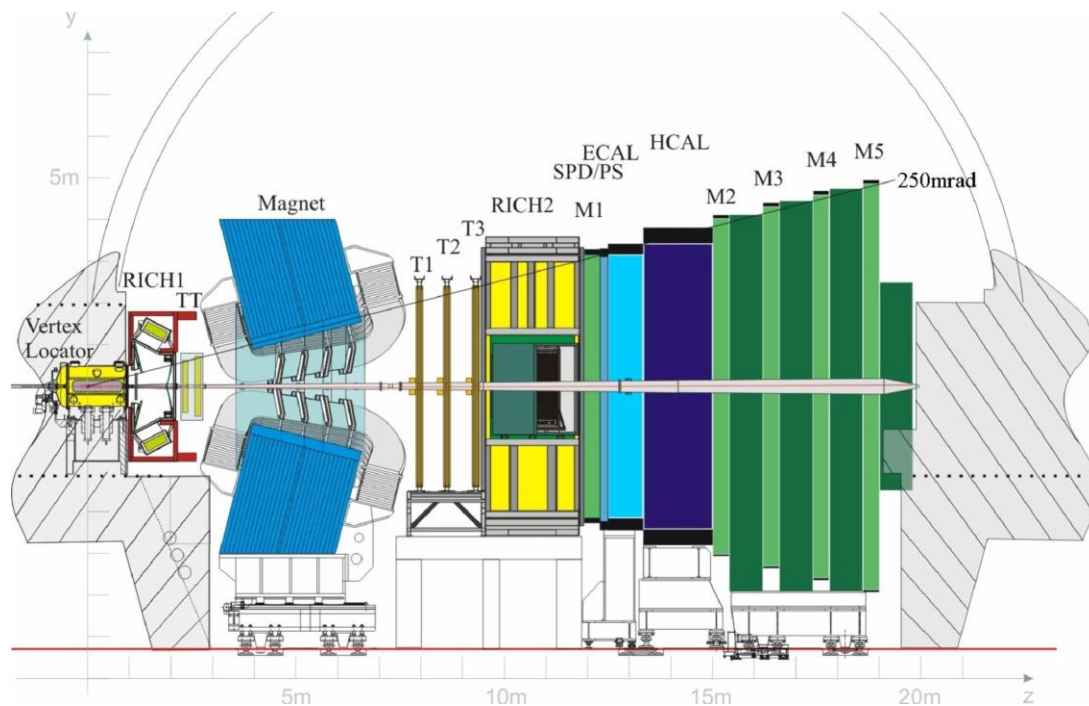
Overview

- The LHCb RICH detectors
- Cherenkov angle resolution and alignment
- Number of photons
- Real-time Online calibration
- PID performance
- Physics impact

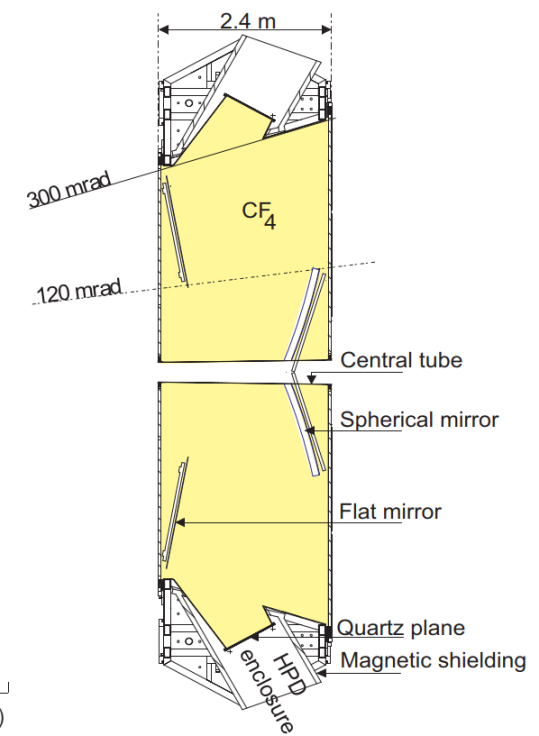
Performance of the LHCb RICH detectors during LHC Run 2
R. Calabrese et al 2022 *JINST* 17 P07013

Performance of the LHCb RICH detector at the LHC
Adinolfi, M. et al. *Eur. Phys. J. C* 73, 2431 (2013).

The LHCb experiment

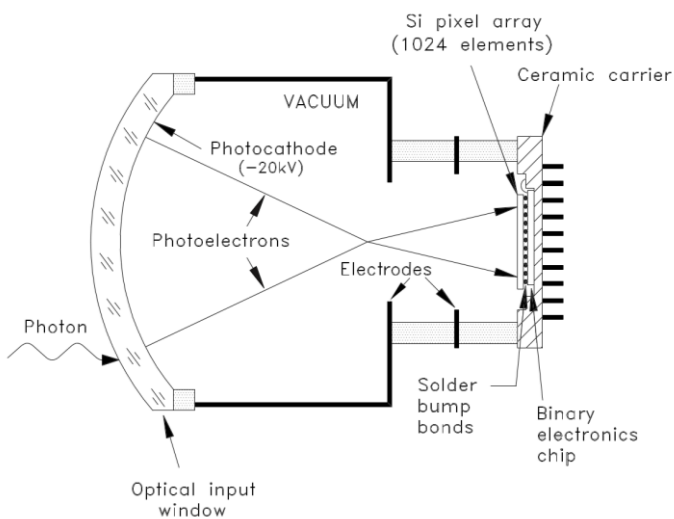


RICH 1



RICH 2

The Pixel Hybrid Photon Detectors

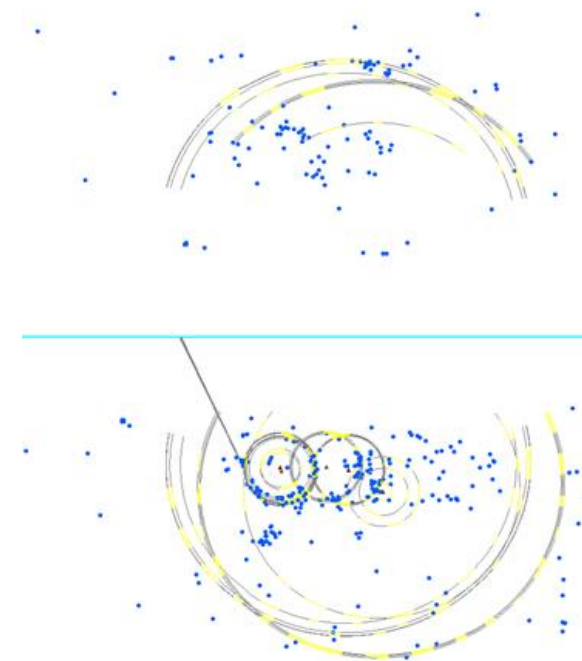


The encapsulated electronics operate at a maximum read-out rate of 1 MHz; not compatible with 40 MHz readout



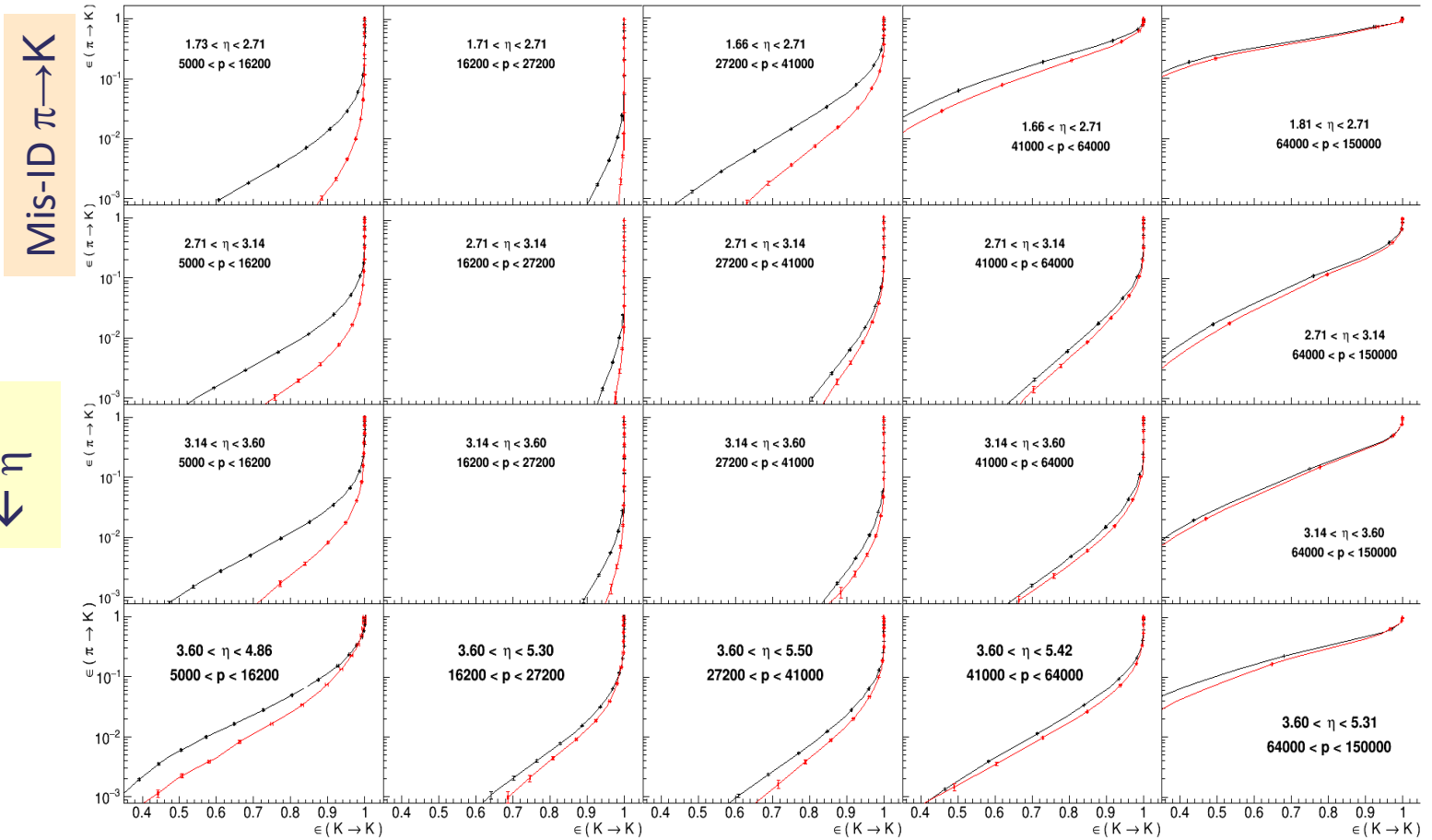
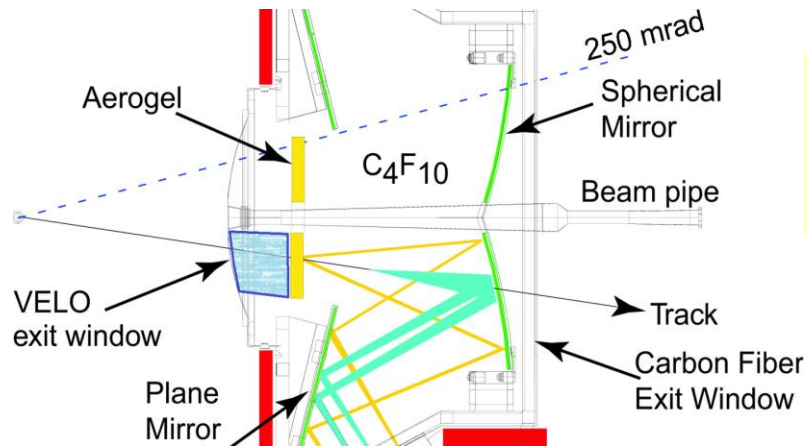
RICH 1: From 2 radiators to 1

- Original design of RICH 1 was to accommodate 2 radiators to cover a wider momentum range:
 - C_4F_{10}
 - Aerogel
- However:
 - Increased luminosity compared to original design and increased background (and underestimate of track multiplicity) made aerogel photons difficult to identify
 - The requirement for offline quality results from High-Level Trigger output put strict conditions for processing time
 - Online alignment and calibration before HLT
- Removal of aerogel extended the length of the gas radiator



Aerogel removal

π/K PID 2012/2015



Mis-ID $\pi \rightarrow K$

$\leftarrow \eta$

Momentum \rightarrow

Efficiency $K \rightarrow K$

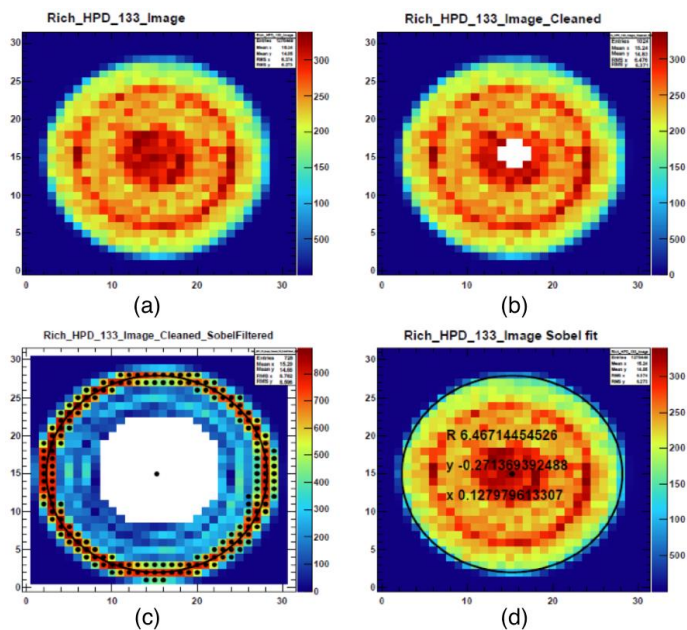


Science and
Technology
Facilities Council

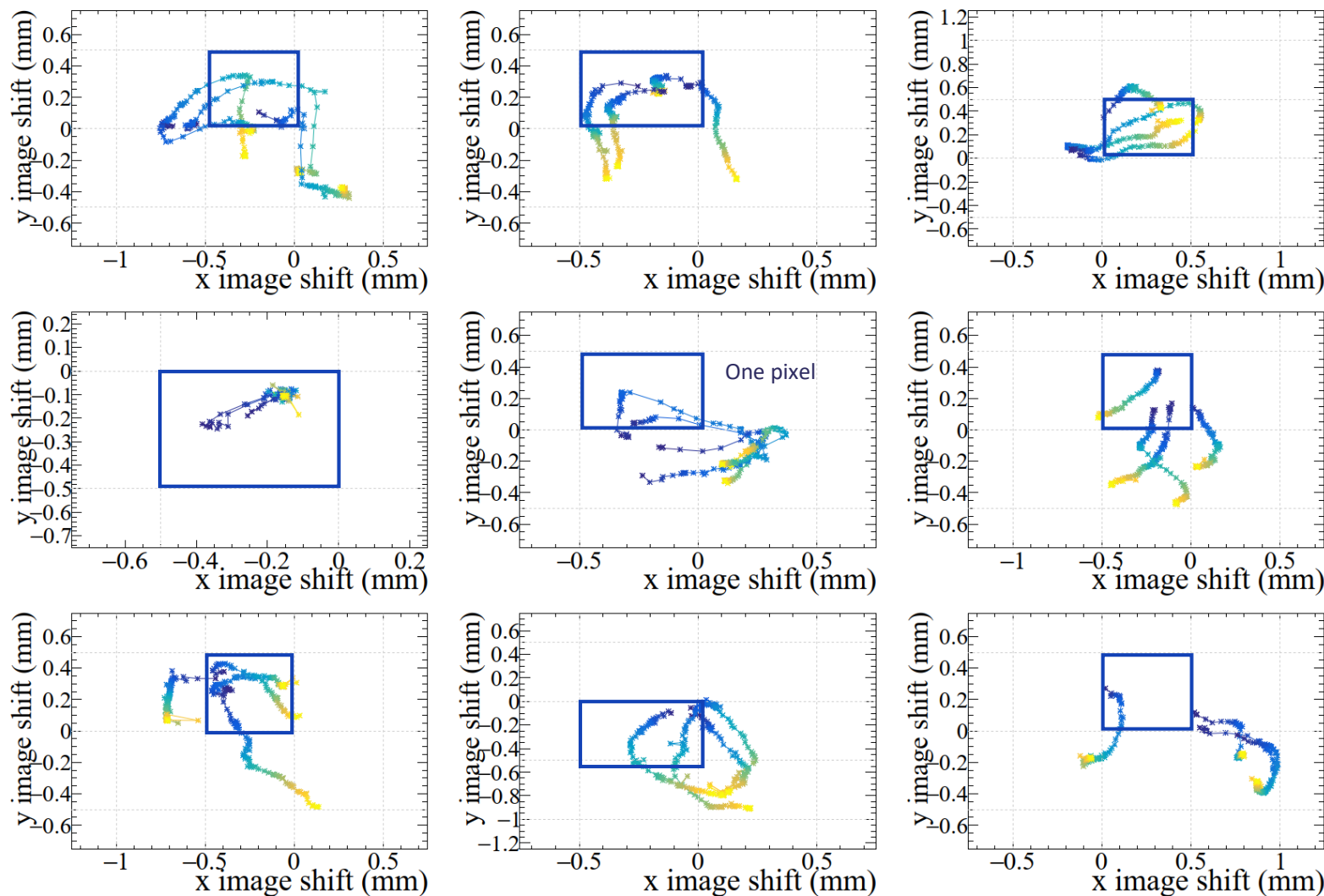
Cherenkov angle reconstruction



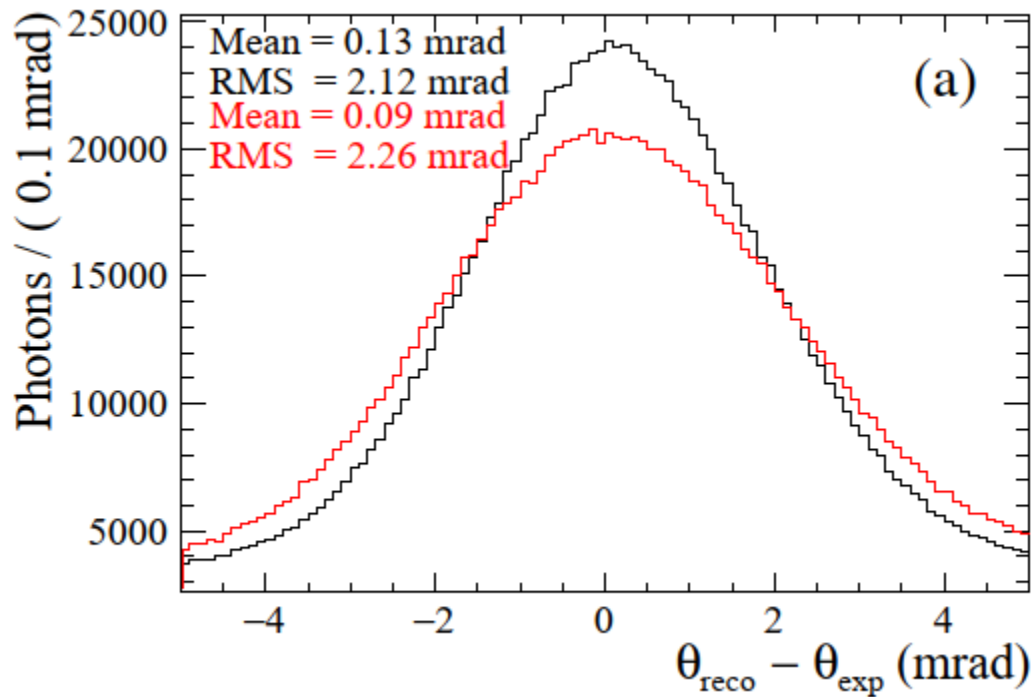
HPD photocathode position



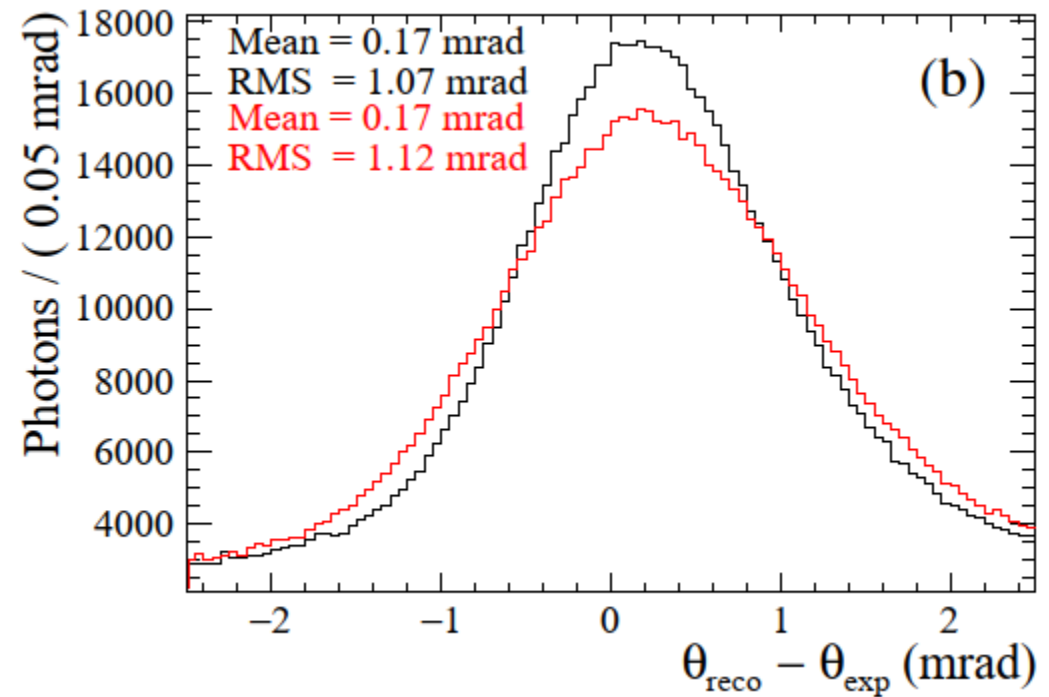
Automatic Online calibration
for every run (max 1 hour)



HPD Image centre effect



RICH 1

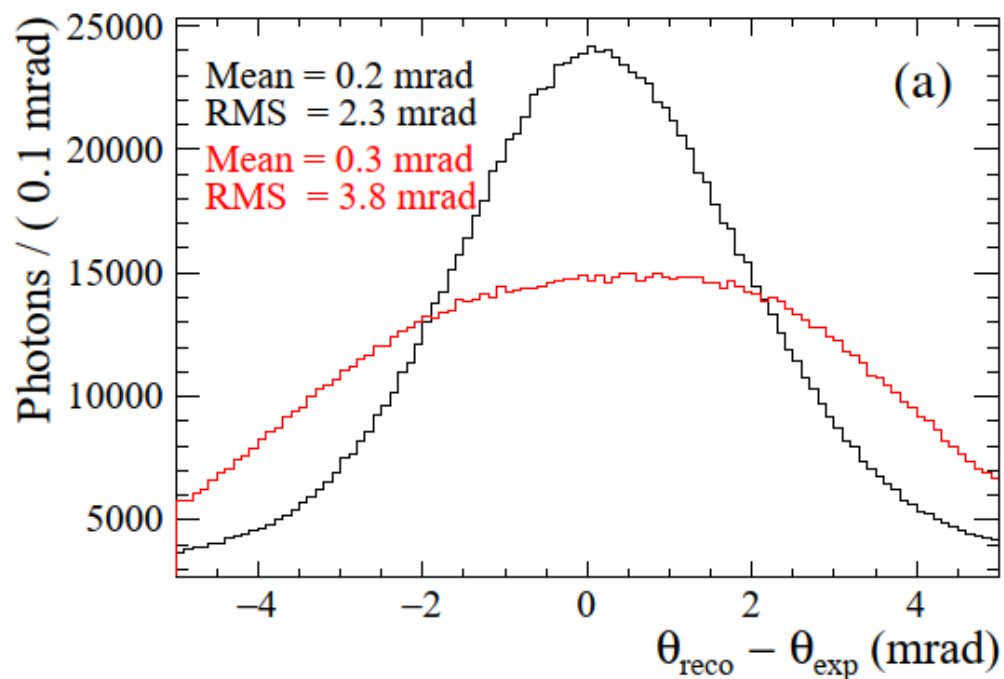


RICH 2

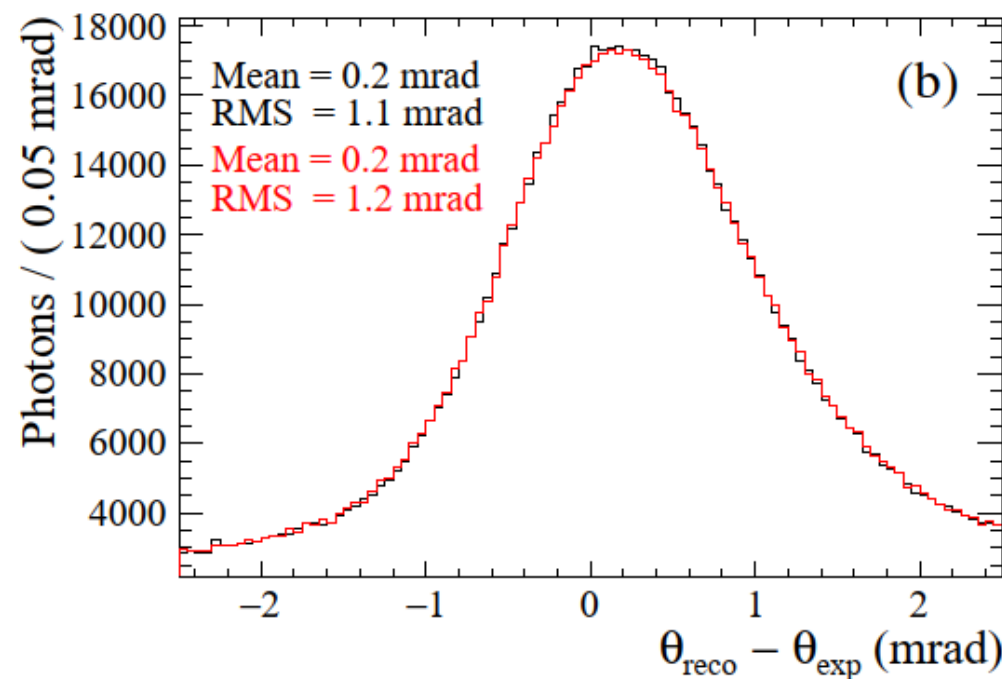
Before corrections

After corrections

Magnetic field distortions

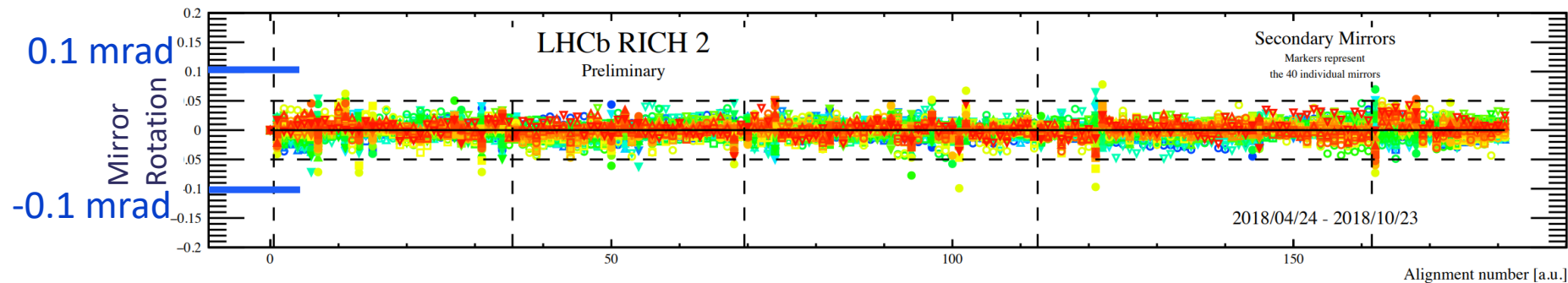
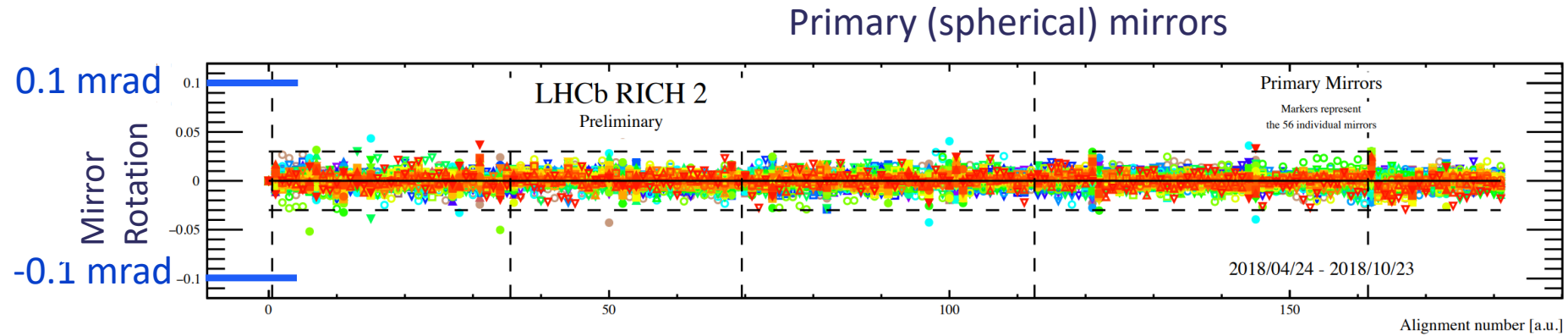
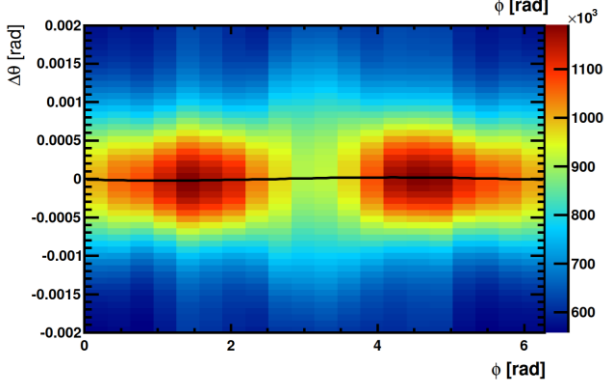
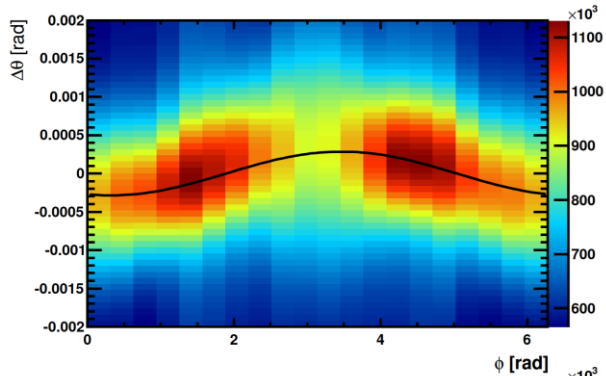


A Borgia *et al*, NIM A 735 (2014) 44-52



R Cardinale *et al*, 2011 JINST 6 P06010

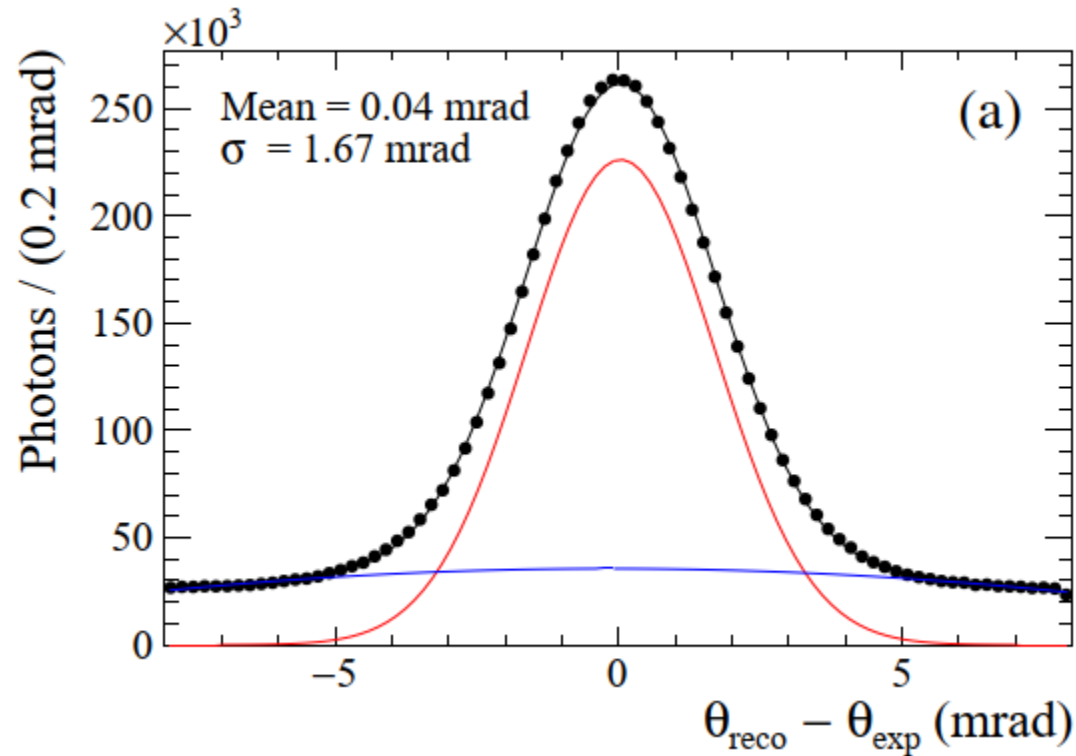
Mirror alignment



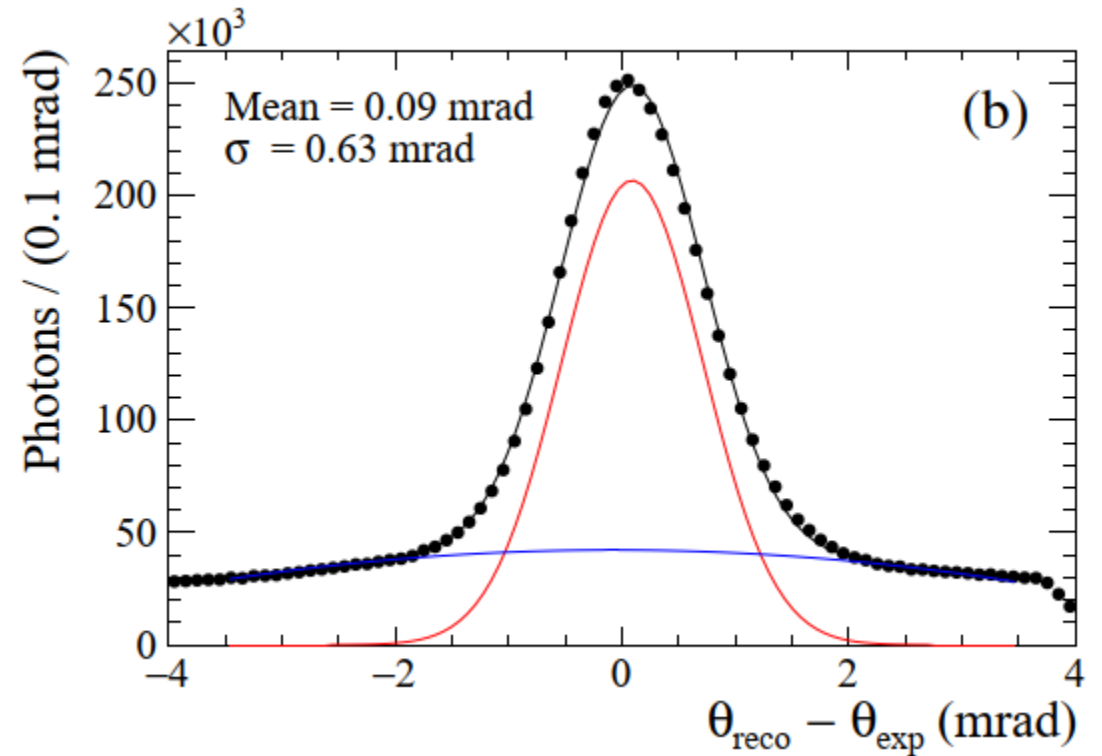
Cherenkov angle resolution



From low track multiplicity events

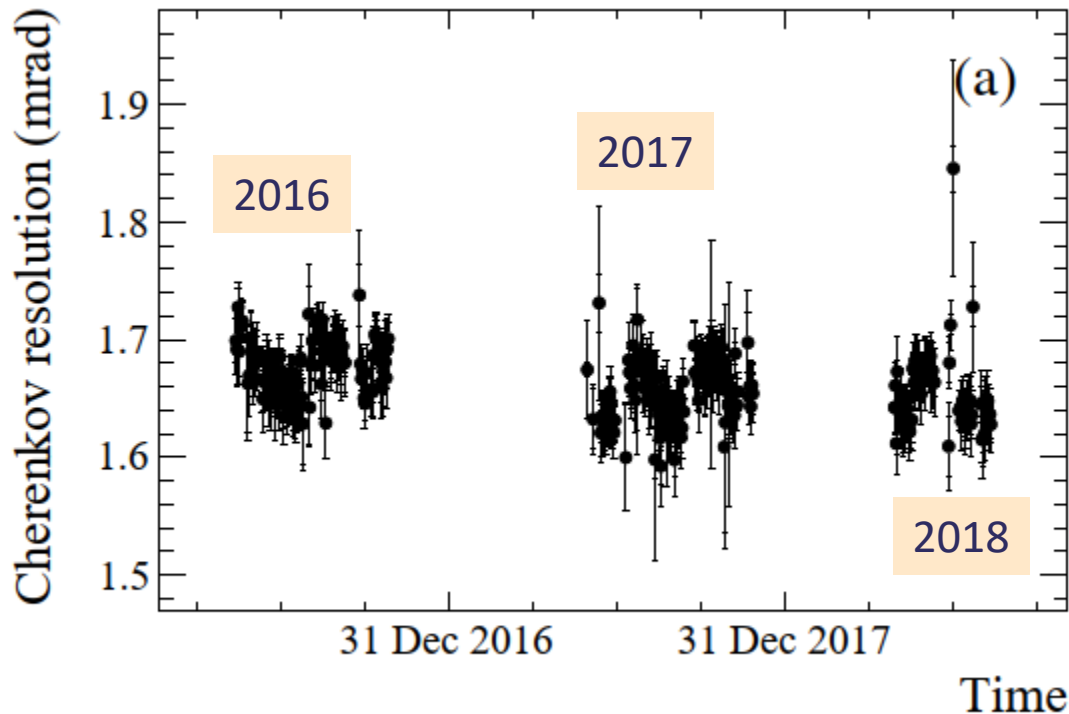


RICH 1

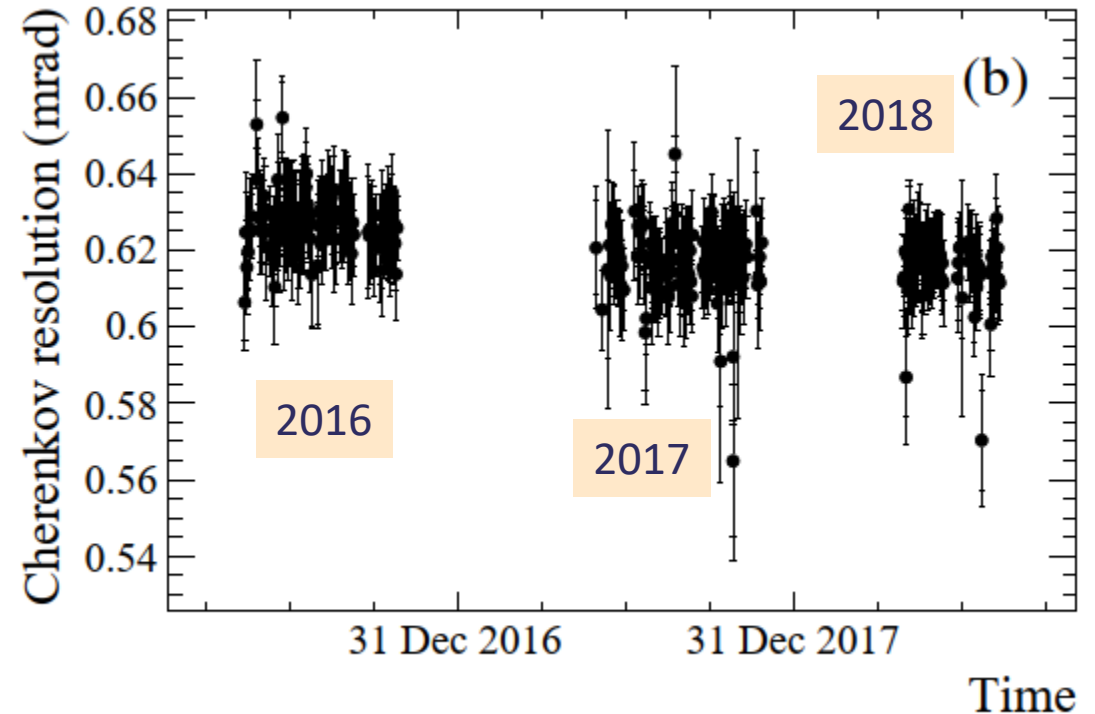


RICH 2

Cherenkov angle resolution stability



RICH 1

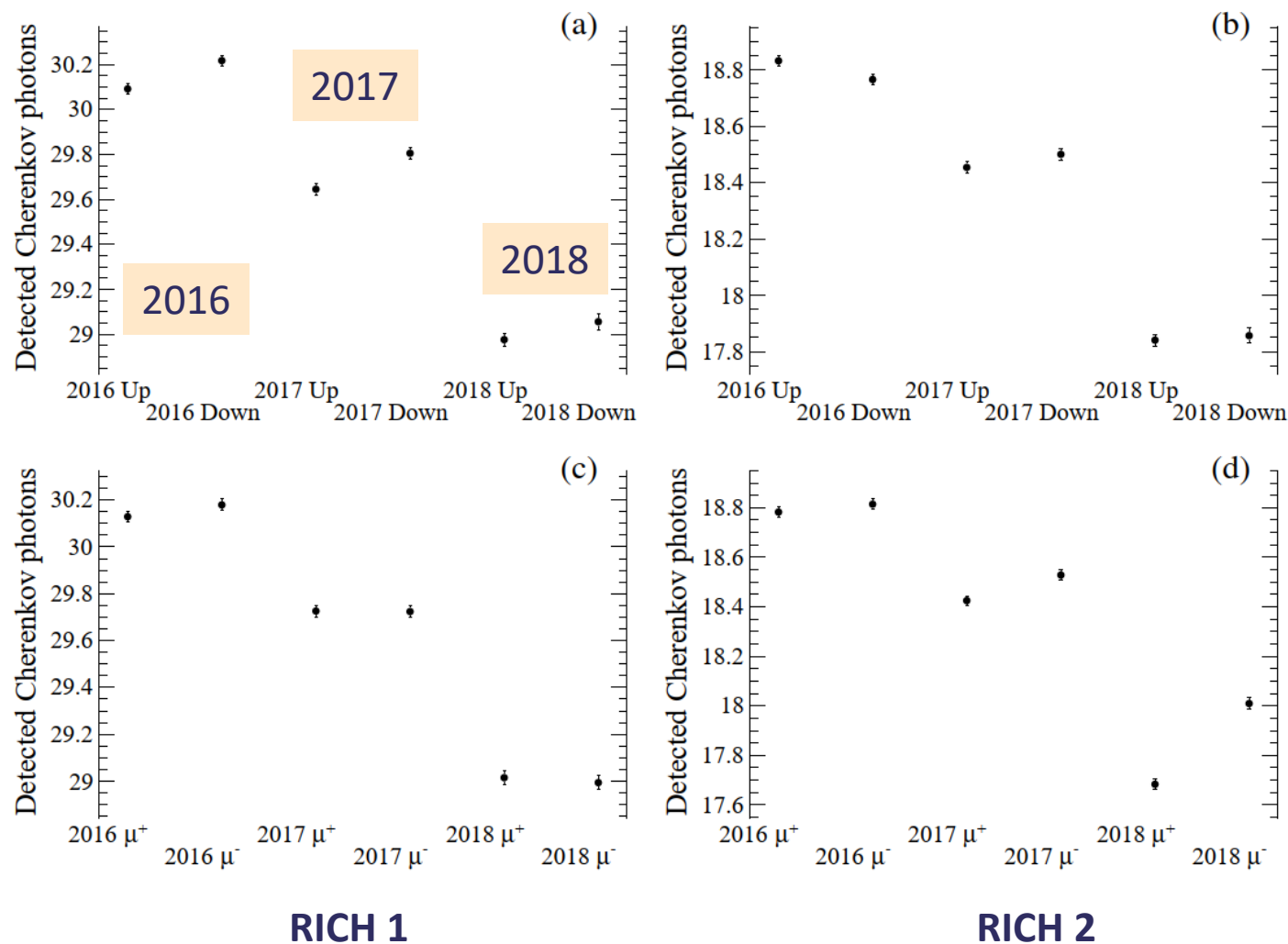


RICH 2

Number of detected photons

Using low multiplicity events, identified as muons by the muon system

The number of photons is estimated per track from the resolution plot with the background subtracted

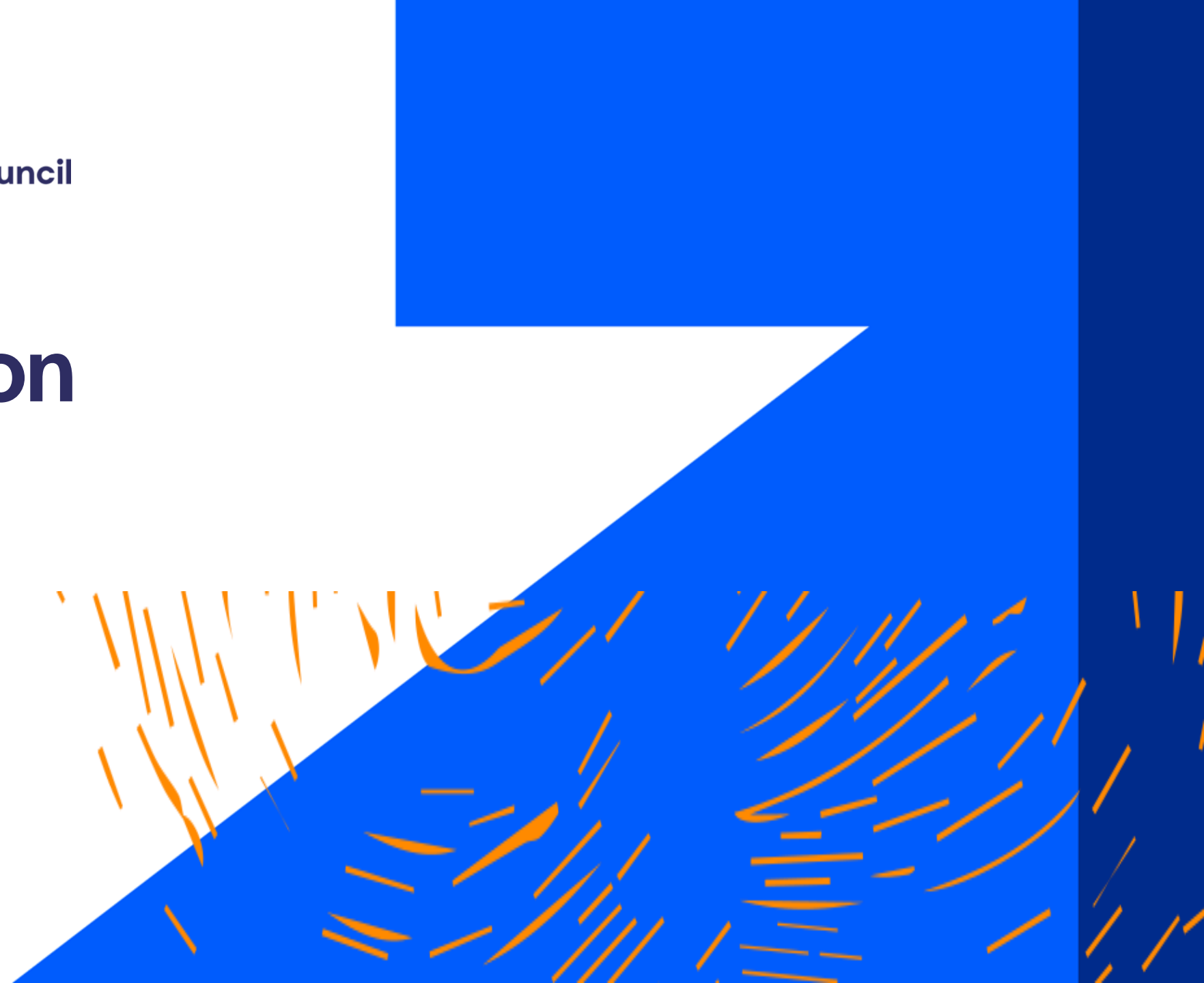


LHCb operates with two magnetic field polarities to avoid systematic errors:
Field UP
Filed DOWN

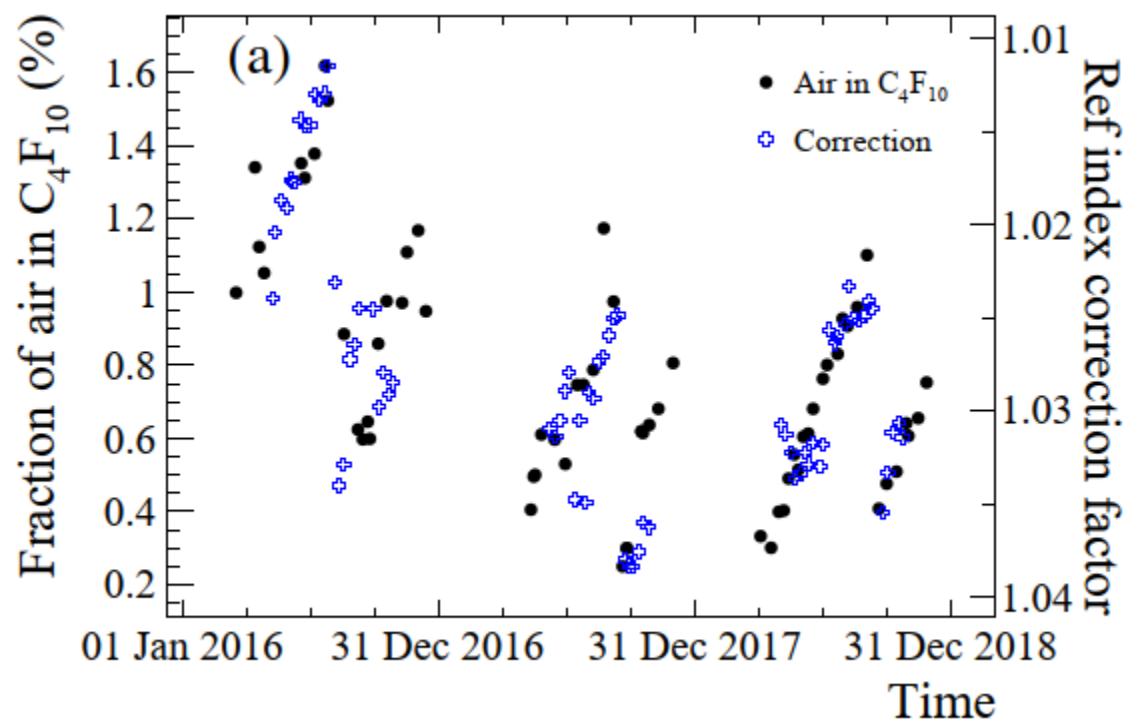


Science and
Technology
Facilities Council

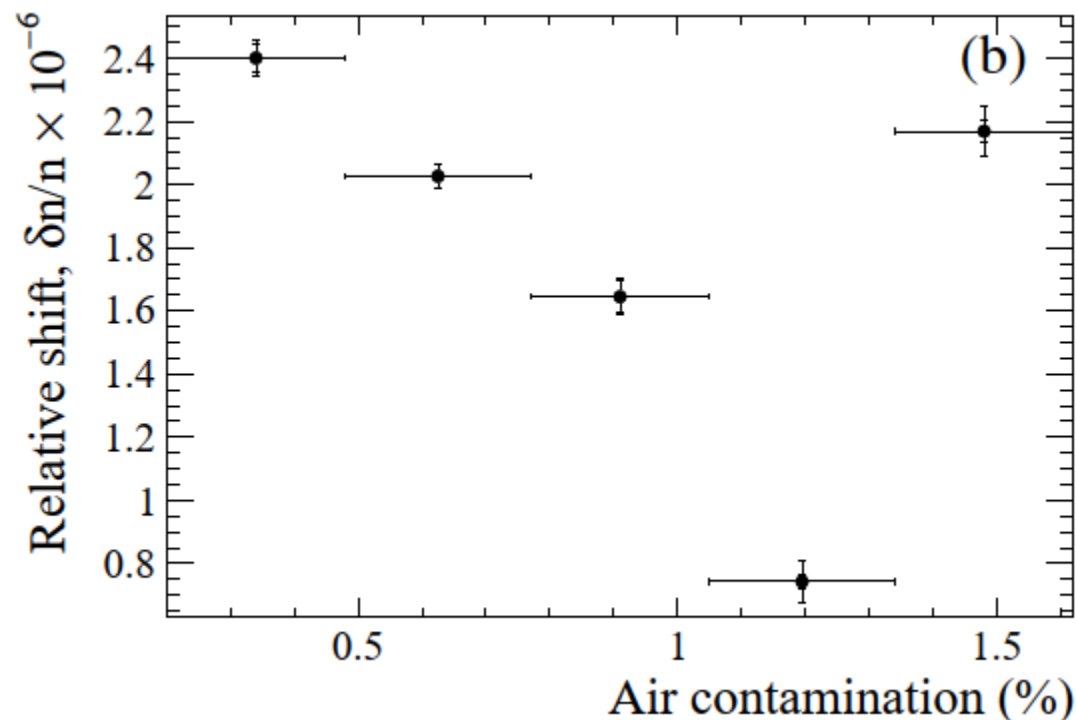
Calibration



Refractive index calibration



Correction factor and air contamination



Residual refractive index bias after correction

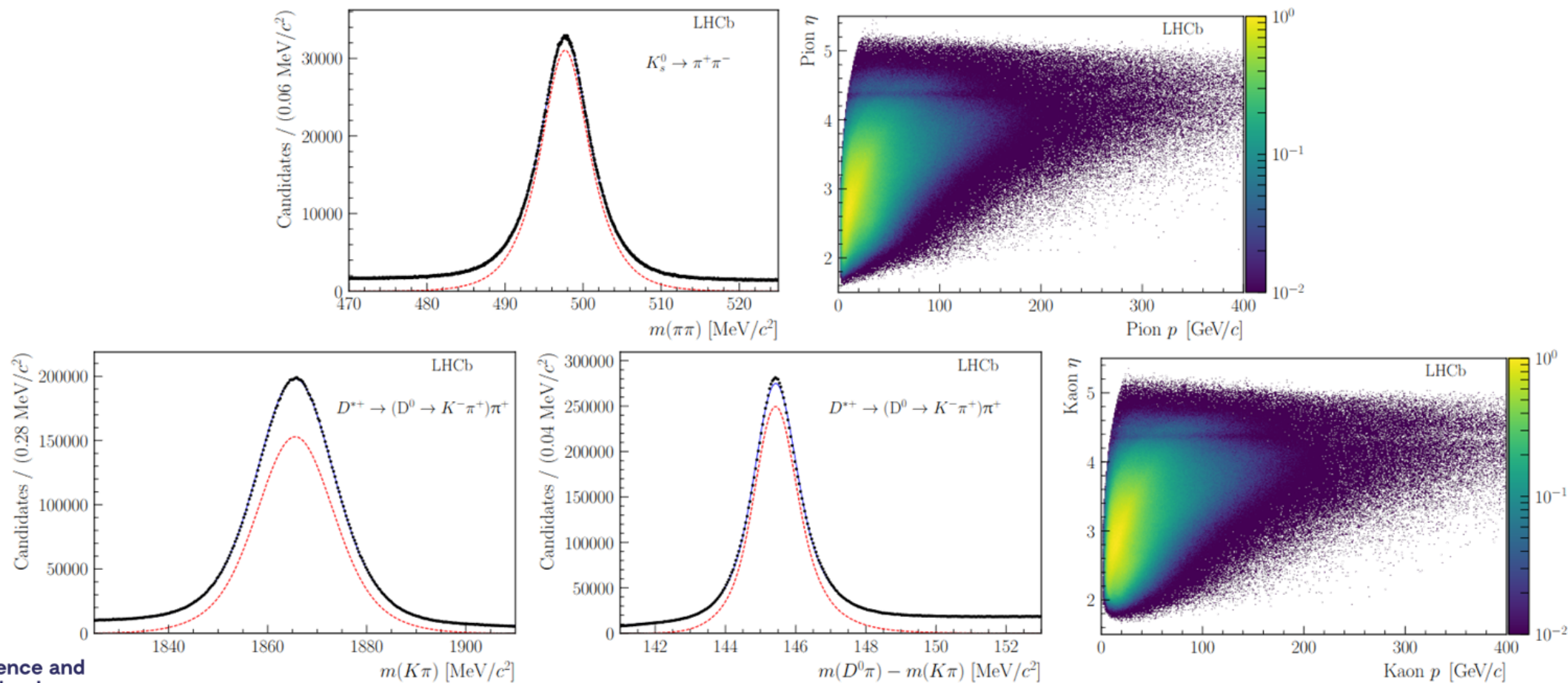
Decays for PID calibration

Identified without RICH information

Species	Low momentum	High momentum
e^\pm	$B^+ \rightarrow J/\psi K^+$ with $J/\psi \rightarrow e^+e^-$	
μ^\pm	$B^+ \rightarrow J/\psi K^+$ with $J/\psi \rightarrow \mu^+\mu^-$	$J/\psi \rightarrow \mu^+\mu^-$
π^\pm	$K_S^0 \rightarrow \pi^+\pi^-$	$D^{*+} \rightarrow D^0\pi^+$ with $D^0 \rightarrow K^-\pi^+$
K^\pm	$D_s^+ \rightarrow \phi\pi^+$ with $\phi \rightarrow K^+K^-$	$D^{*+} \rightarrow D^0\pi^+$ with $D^0 \rightarrow K^-\pi^+$
p, \bar{p}	$\Lambda^0 \rightarrow p\pi^-$	$\Lambda^0 \rightarrow p\pi^-$; $\Lambda_c^+ \rightarrow pK^-\pi^+$

EPJ Techn Instrum 6, 1 (2019). <https://doi.org/10.1140/epjti/s40485-019-0050-z>

Kinematic range (K, π)





Science and
Technology
Facilities Council

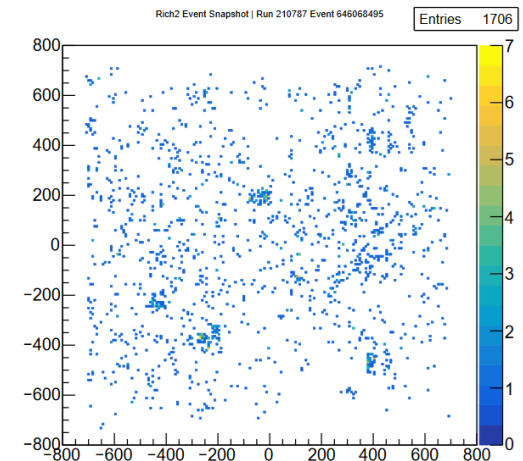
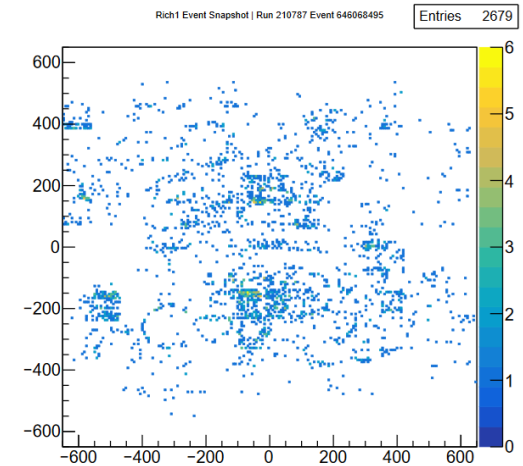
PID performance



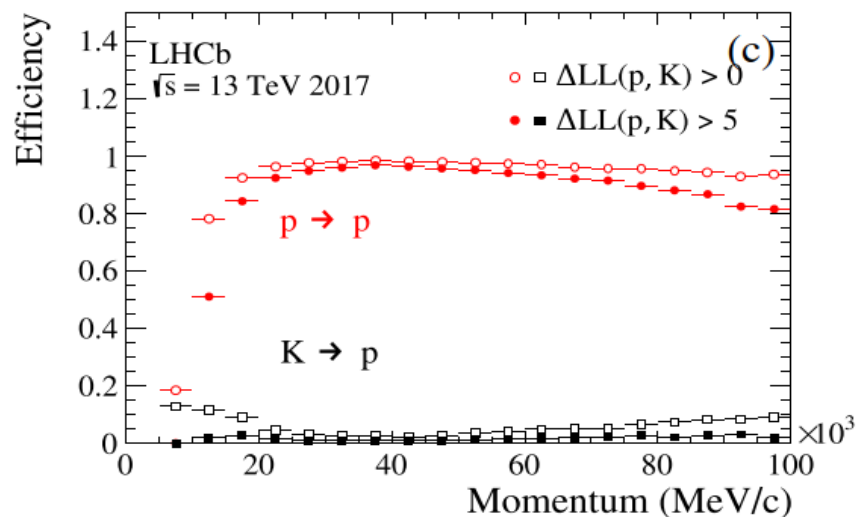
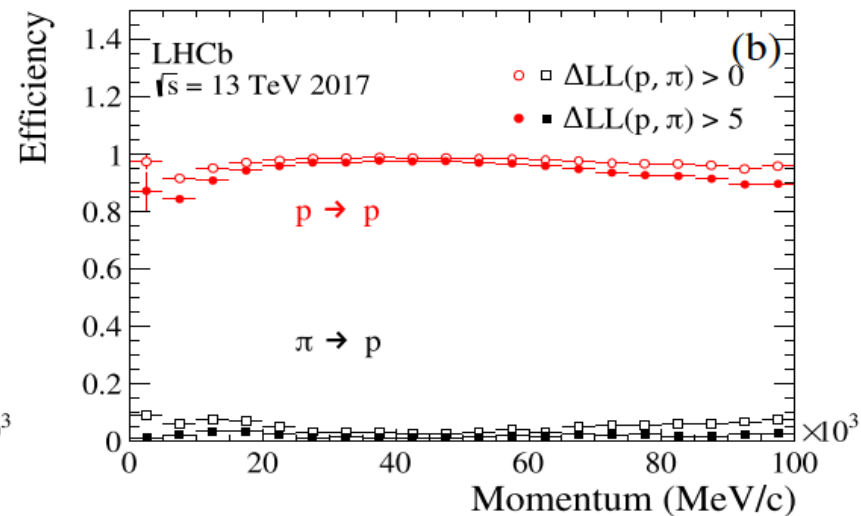
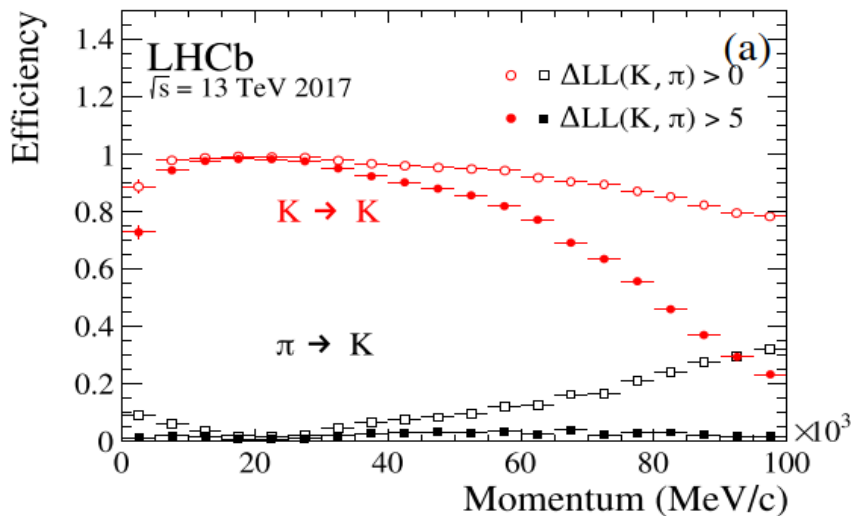
Global likelihood PID method



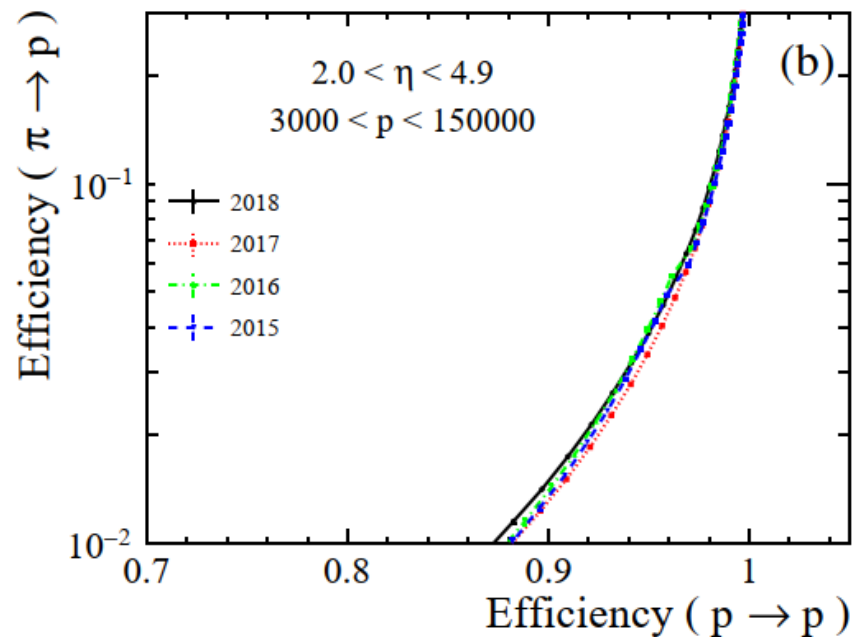
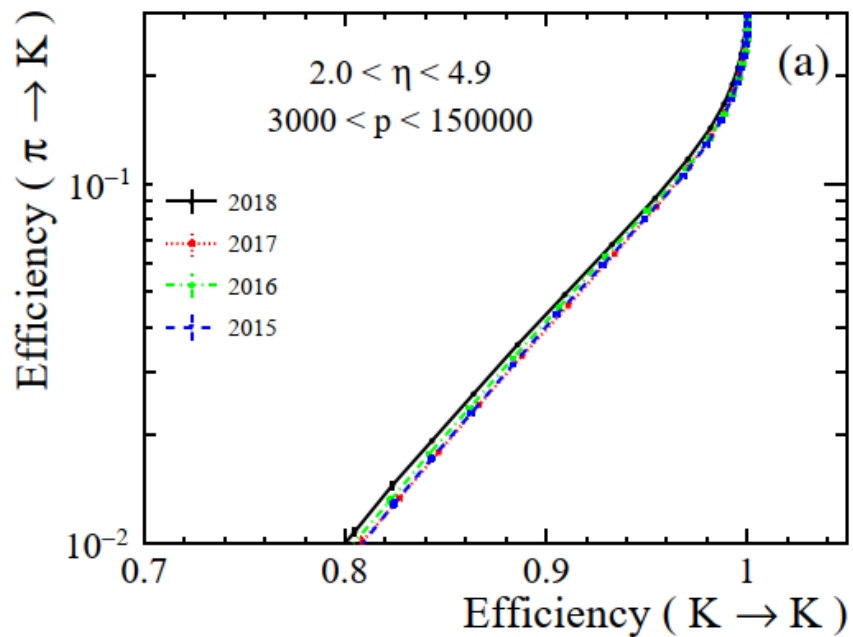
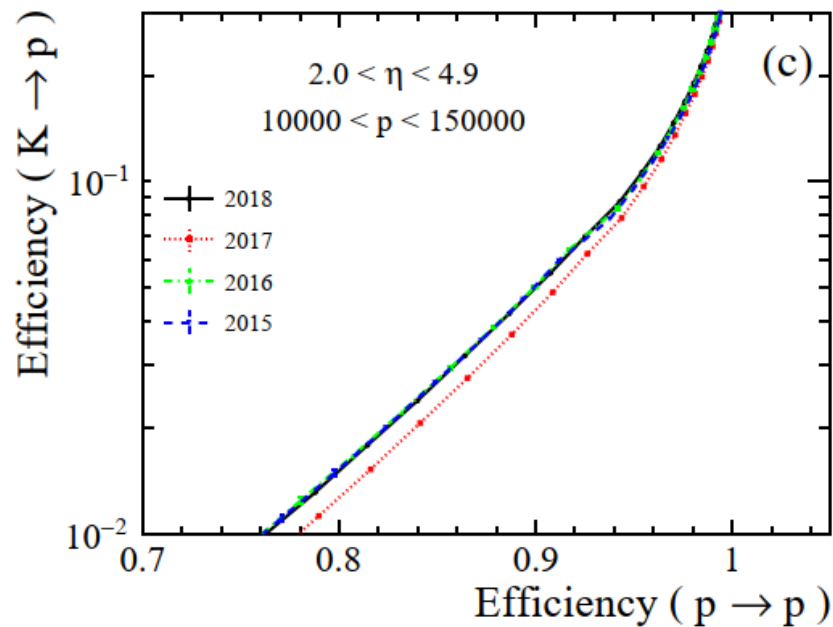
- In the busy LHC environment, most of the “background” to the identification of a given track comes from signals of other tracks in the event
 - [make a global optimisation of the mass hypotheses](#)
- For each track in the event, for a given mass hypothesis, determine the expected distribution of Cherenkov photons on the detector plane using the knowledge of the geometry of the detector and its optical properties
- Repeat for all the tracks in the event
- From the photon distribution on the detector plane calculate the probability that a signal would be seen in each pixel of the detector from all tracks
- Compare this with the observed set of photoelectron signal on the pixels and calculate a likelihood
- Repeat the above, changing the set of mass hypothesis of the tracks to find the set of mass hypotheses which maximize the likelihood



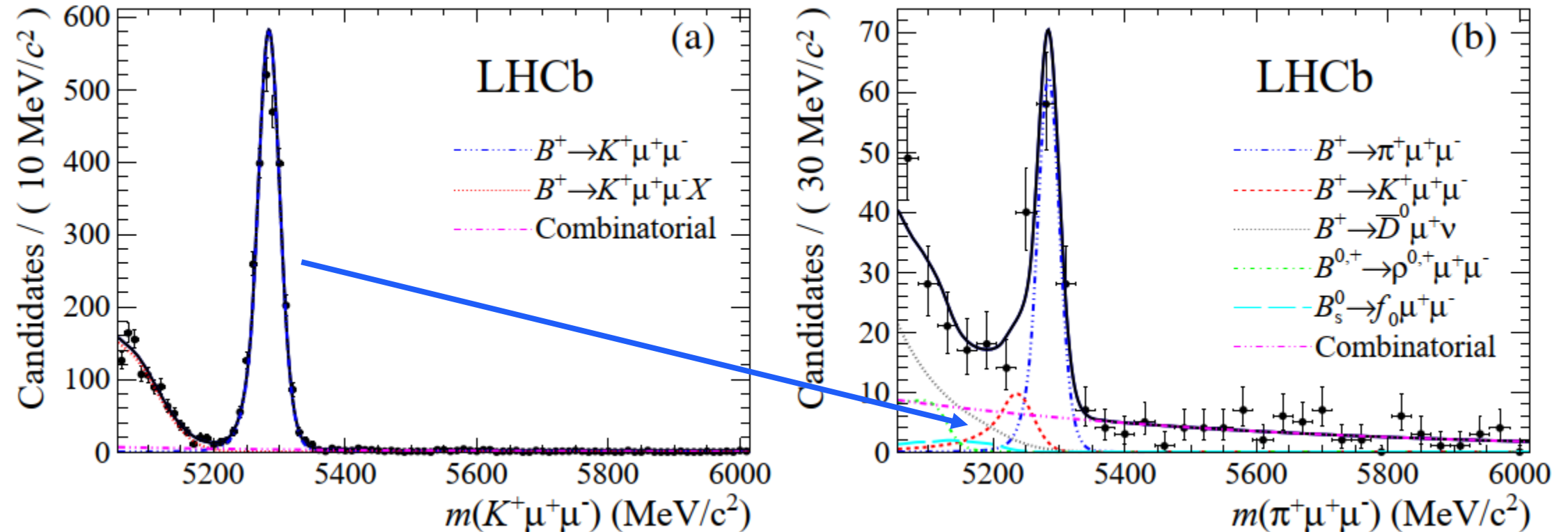
PID performance (2017)



PID stability



Physics impact of hadron PID



First measurement of the differential branching fraction and CP asymmetry of the $B^\pm \rightarrow \pi^\pm \mu^+ \mu^-$ decay, JHEP 10 (2015) 034 [arXiv:1509.00414]

Summary



- The data from years 2016 to 2018 have been analysed leading to a better understanding of the detectors and knowledge towards future designs
- The original LHCb RICH detectors have been replaced with the new upgraded versions
 - Brand new RICH 1, new photon detectors and new electronics everywhere
- This is an opportunity to celebrate the success of the original design showing the exceptional performance and stability in a difficult hadron environment



LHCb Upgrade of the RICH Detectors

Antonino Sergi
University of Genova and INFN
on behalf of the LHCb RICH collaboration

**11th International Workshop on Ring Imaging Cherenkov Detectors
"RICH 2022"**

RICH Upgrade

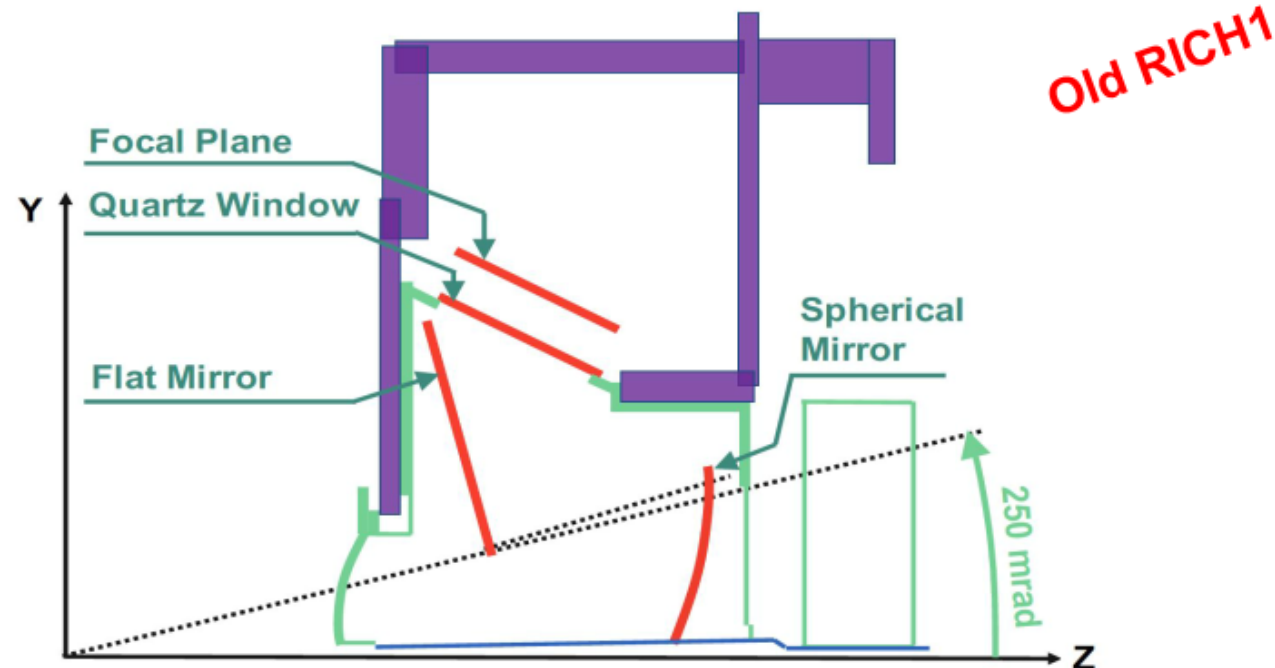
LHCb

- Adapt the current RICH detectors to run at higher luminosity and with continuous 40 MHz read-out
- Mechanical and optical changes
 - RICH1 spherical mirrors focal length increased to reduce occupancy (optical system re-designed)
 - New support mechanics and cooling
- Electronics and data acquisition changes
 - Replace HPDs with commercial MultiAnode PhotoMultiplier Tubes (MaPMTs) with 64 channels
 - Use 40 MHz front-end electronics and data acquisition
 - CLARO8 amplifier/discriminator ASIC
 - FPGA-based digital board
 - GigaBit Transceiver (GBT) chip for data transmission

New Mechanics

LHC6

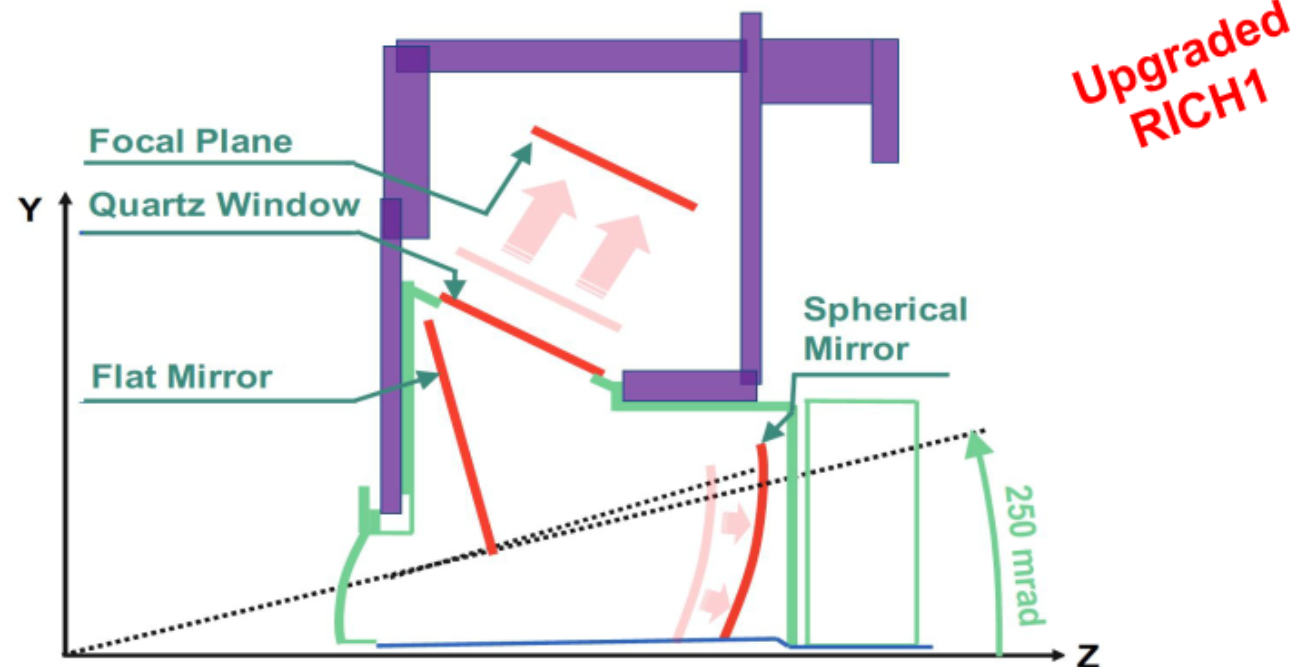
- Peak occupancy should remain $< 30\%$ to maintain PID performance
- Focal plane and spherical mirror moved back to increase ring size
- New spherical mirrors with larger curvature radius
- Larger gas enclosure
- Compact photo-detection system required



New Mechanics

LHC6

- Peak occupancy should remain $< 30\%$ to maintain PID performance
- Focal plane and spherical mirror moved back to increase ring size
- New spherical mirrors with larger curvature radius
- Larger gas enclosure
- Compact photo-detection system required



MultiAnode PhotoMultipliers

LHCb

- Hamamatsu MaPMTs
 - 3100 R13742 and 450 R13743, including spares
 - Super-bialkali photocathode
 - UV glass window
 - Minimum gain 1×10^6 at 1 KV
 - 1:4 pixel gain spread in 1" PMTs, 1:3 pixel gain spread in 2" PMTs
 - Low dark count rate
 - Single photon spectrum well separated from the noise pedestal
- Higher QE of MaPMT in the green
 - Chromatic error reduction
- Sensitive to magnetic fields
 - Shielding applied

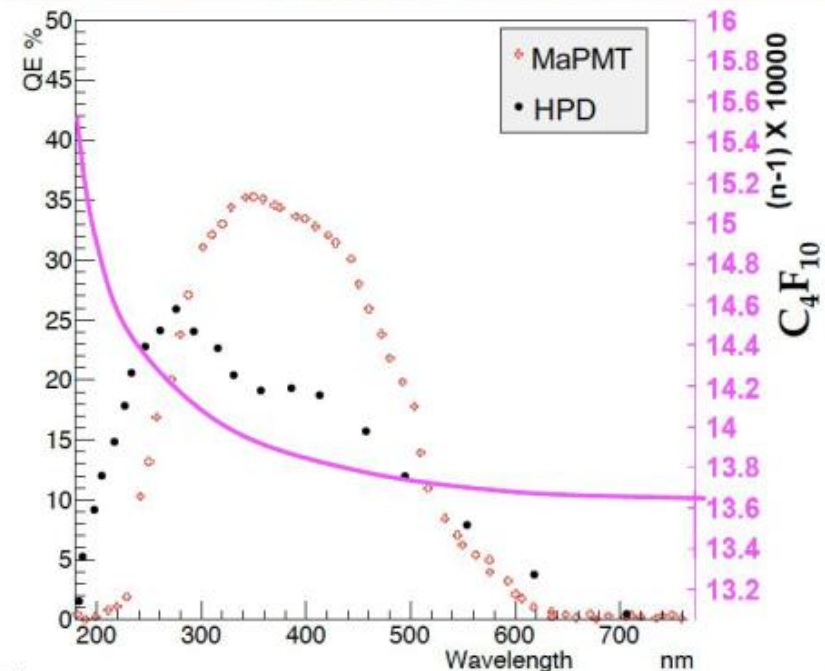
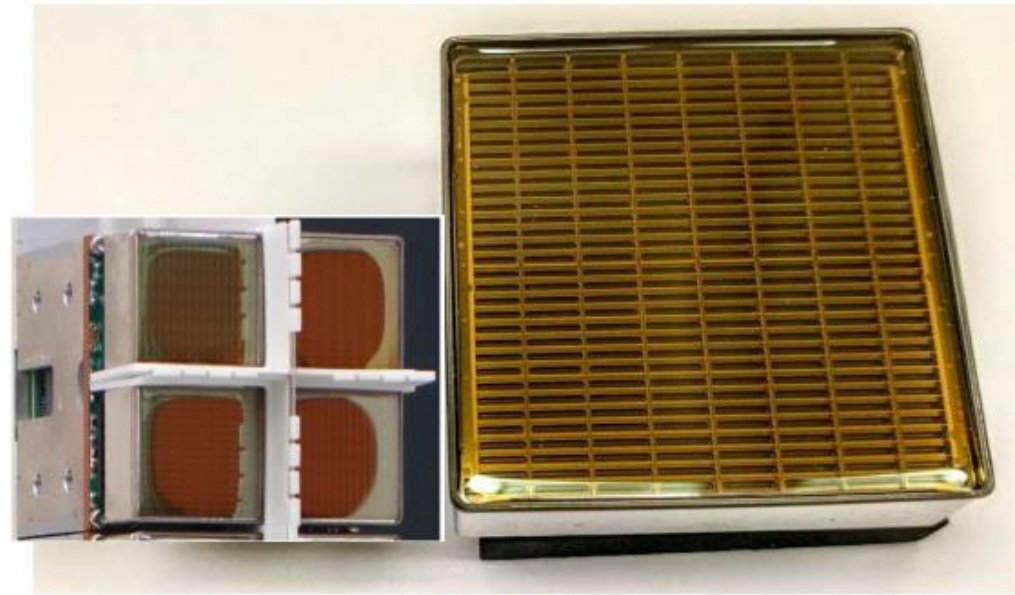


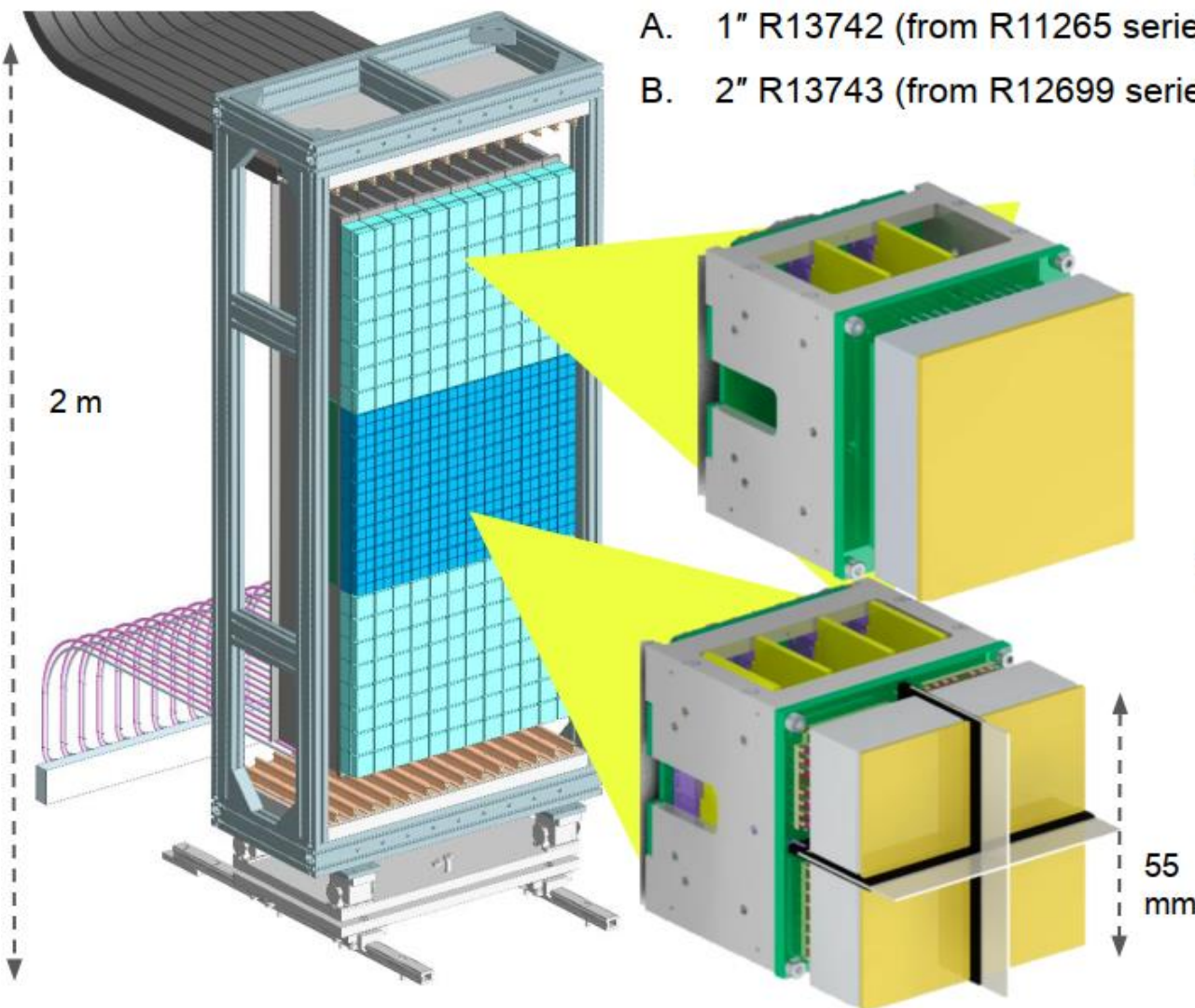
Photo-Detector Assembly

LHCb

I. Hamamatsu MaPMTs with 8×8 pixel matrix, arranged in Elementary Cells (EC)

A. 1" R13742 (from R11265 series)

B. 2" R13743 (from R12699 series)

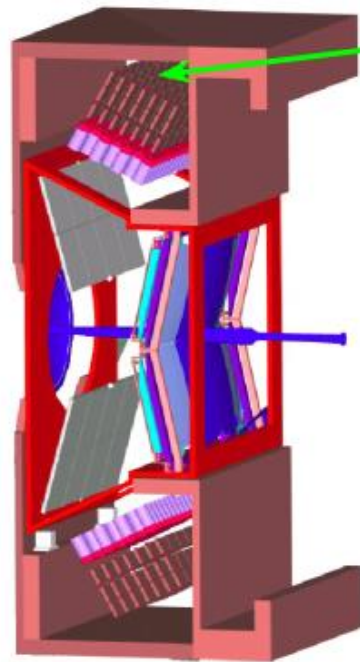


- EC-H type: 2" MaPMT
 - ~400 modules
 - Outer regions of RICH2
 - One "A" MaPMT per EC (larger model 2×2 inches)
- EC-R type: 4×1" MaPMTs
 - 2×2 matrix of "B" MaPMT per EC (smaller module 1×1 inches)
 - ~ 2700 MaPMT
 - ~ 700 modules
 - RICH1 and central region of RICH2

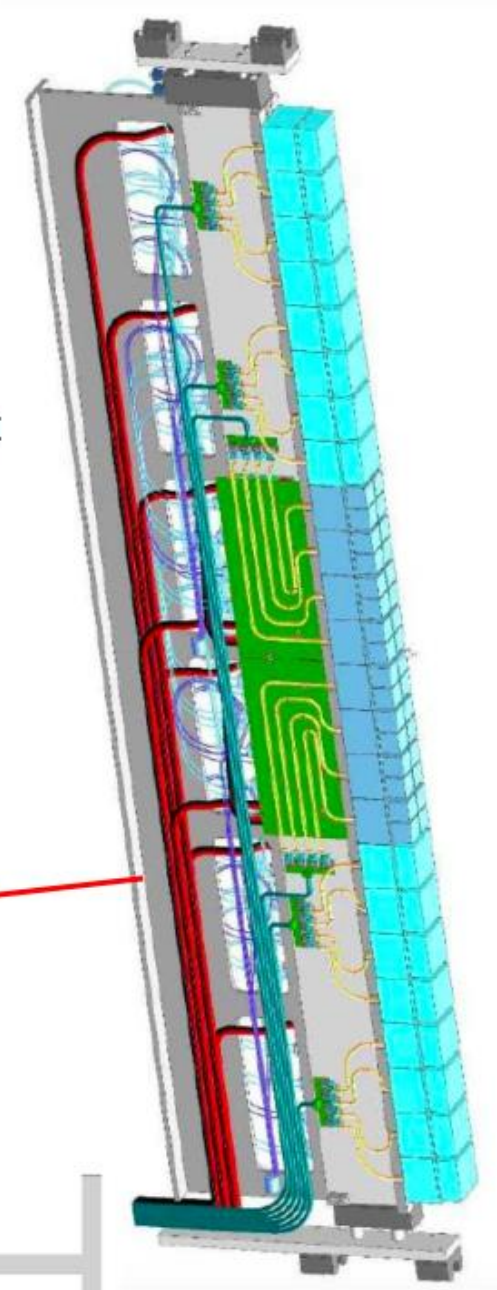
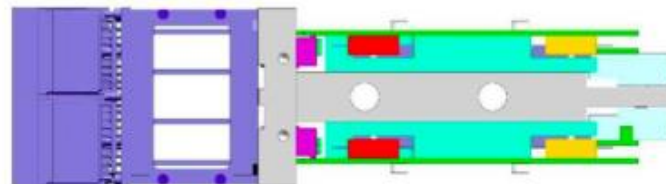
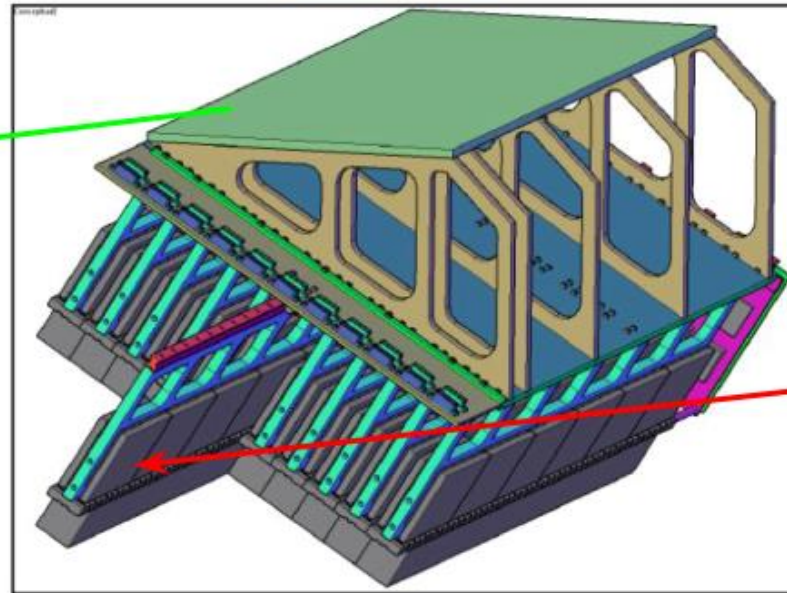
Columns

LHCb

- Mechanical support for Elementary Cells, PDMDB, harness and cooling
 - Easy to remove a column for maintenance
 - Same mechanical structure for columns in RICH1 and RICH2 but different supports



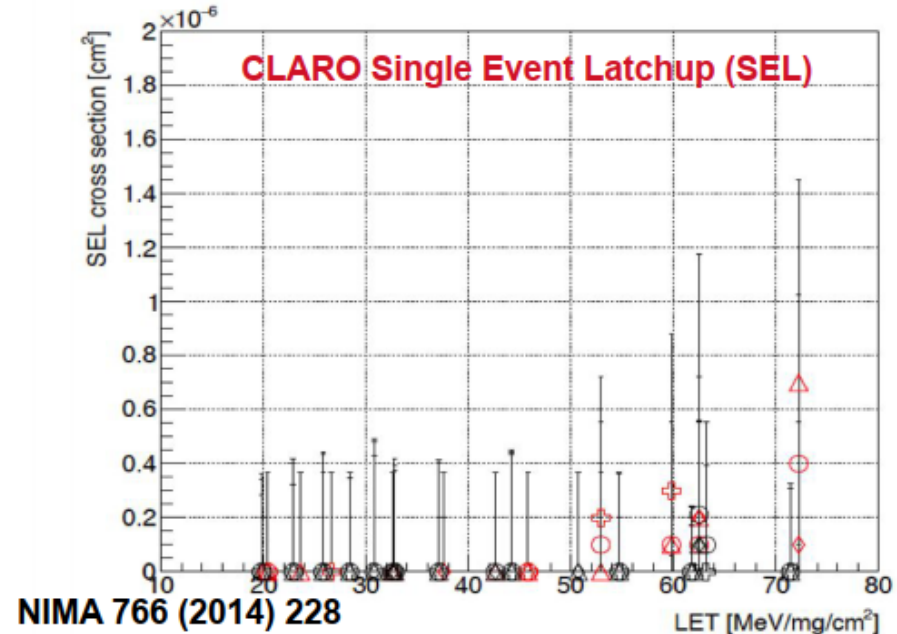
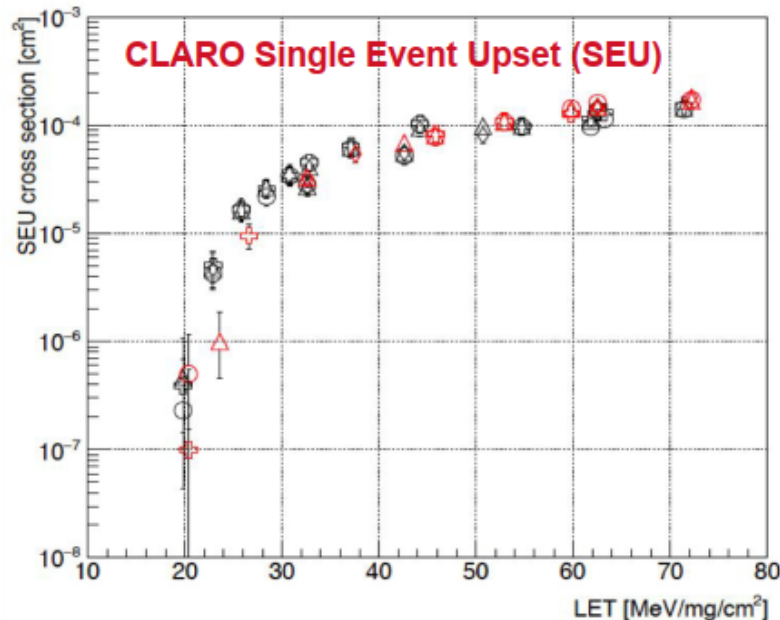
Translation of a column



Radiation Hardness

LHCb

- High radiation levels expected for whole upgrade phase (50 fb^{-1}) at the RICH photodetector plane location
 - 200 krad , $3 \times 10^{12} \text{ 1 MeV } n_{\text{eq}}/\text{cm}^2$, $1.2 \times 10^{12} \text{ HEH}/\text{cm}^2$
- The read-out (CLARO and FPGA) have been tested for Single Event Effects (SEE) and Total Ionizing Dose (TID)
 - CLARO uses radiation-hard by design cells (IMS-CNM Sevilla)
- Xilinx Kintex-7 FPGA is suitable for operation in LHCb RICH
 - Periodic scrubbing foreseen for error mitigation



NIMA 766 (2014) 228

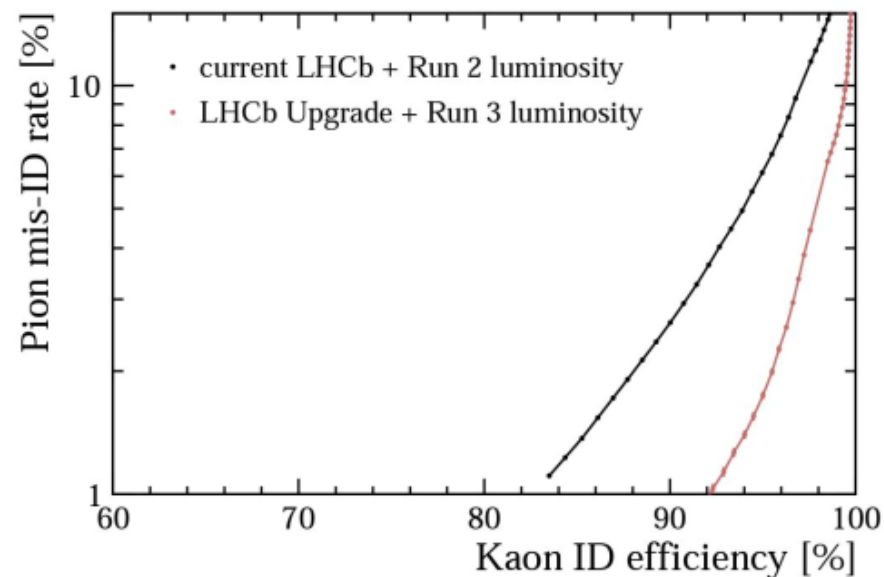
Estimated performance

LHCb

	Photon yield		Cherenkov angle resolution [mrad]				
	$N_{\text{ph}}^{\text{optimal}}$	$N_{\text{ph}}^{\text{typical}}$	chromatic	emission point	pixel	σ_{θ}	$\Delta\theta_{\text{C}}$
RICH1	63	59	0.52	0.36	0.50	0.81	0.18
RICH2	34	30	0.34	0.32	0.22	0.52	0.17

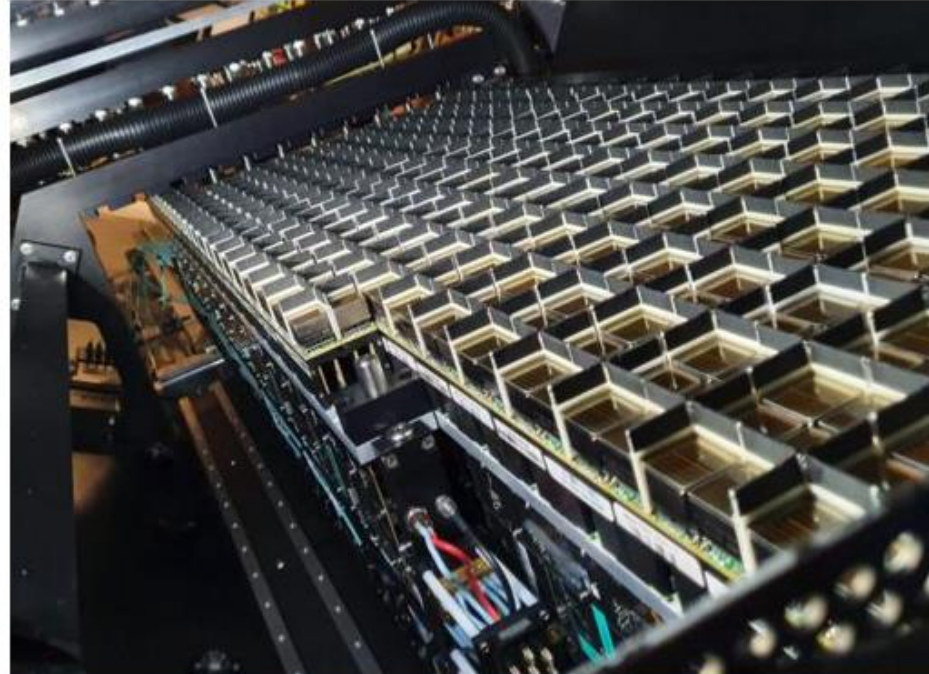
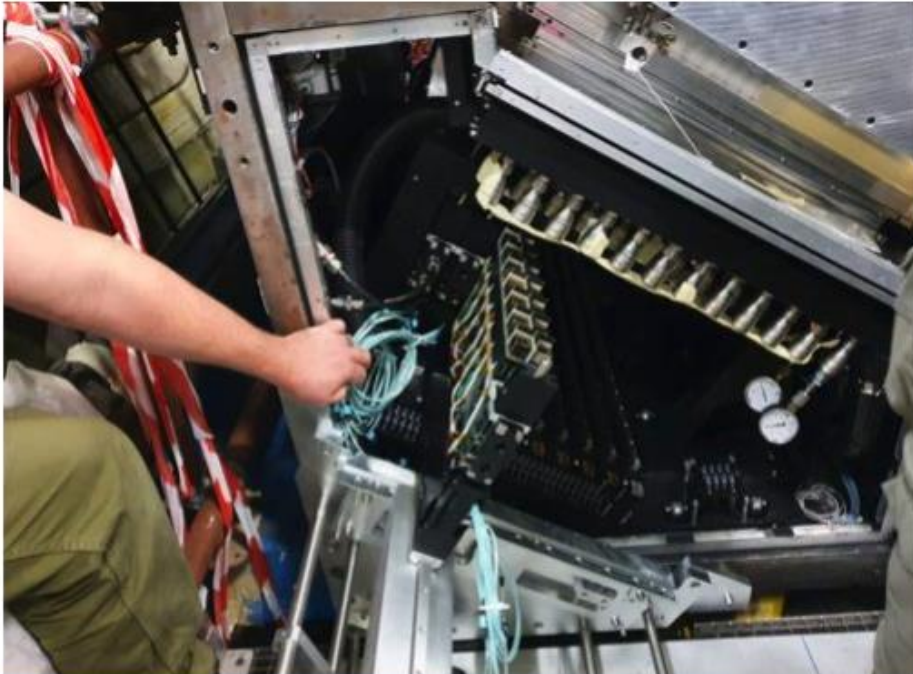
Included in the current simulation

- All measured parameters of optical components
- All feedback from test beams and commissioning
- Experience from the simulation of the previous implementation of this detector



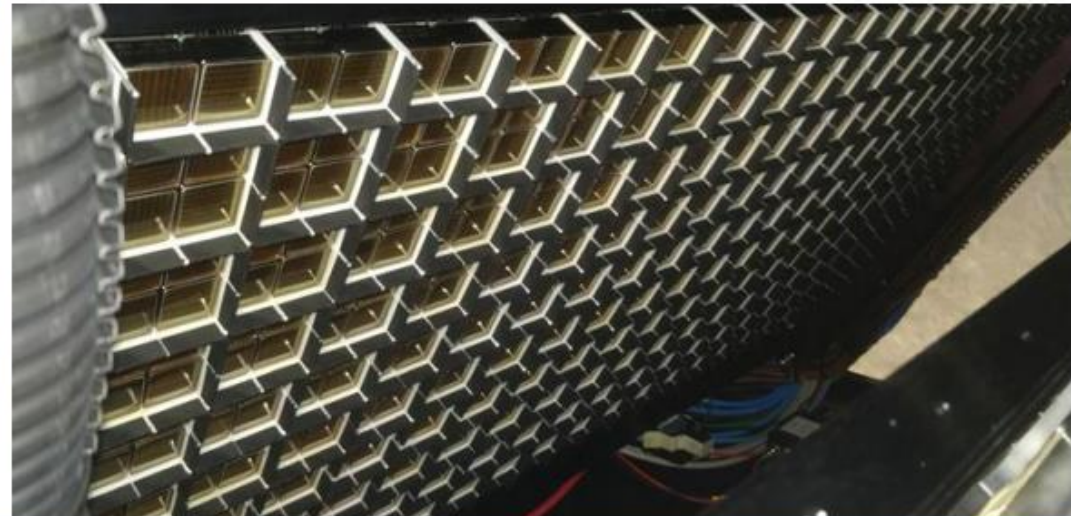
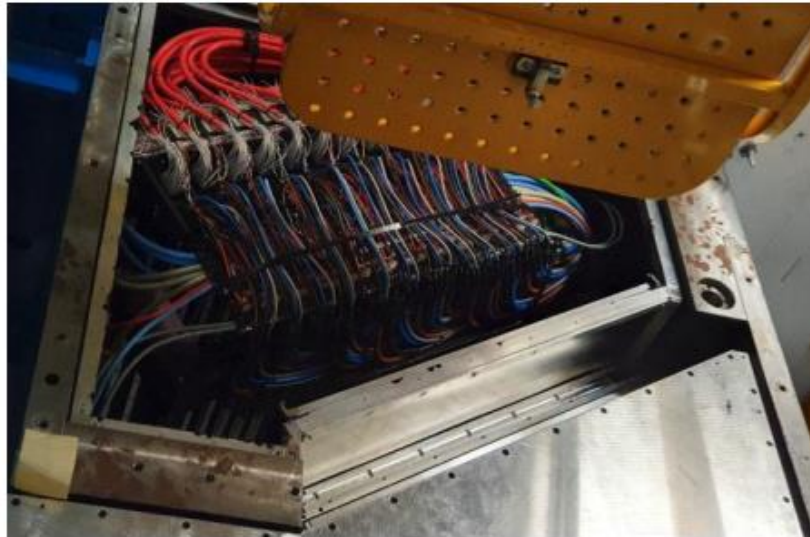
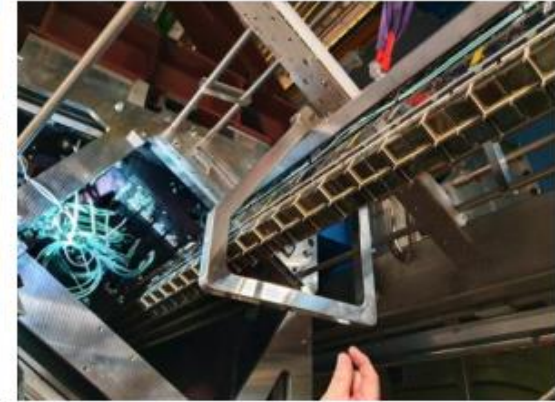
RICH1 Installation: Down Box (12/2021)

LHC6



RICH1 Installation: Up Box (01/2022)

LHC6

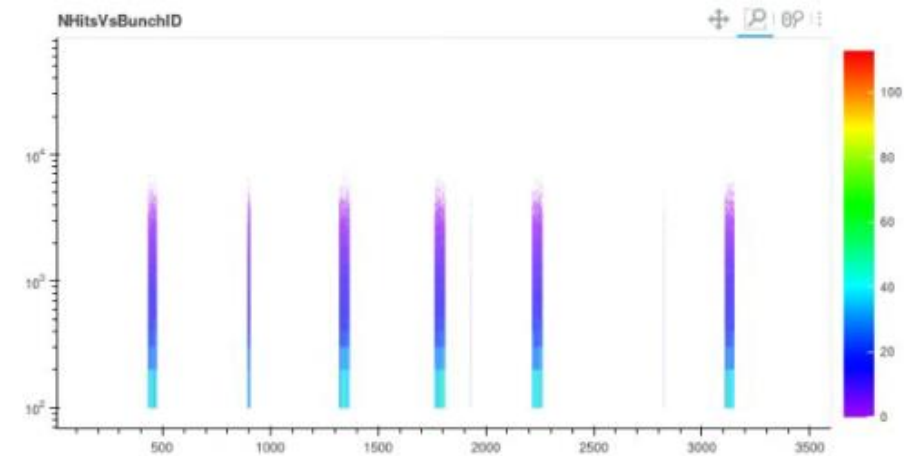
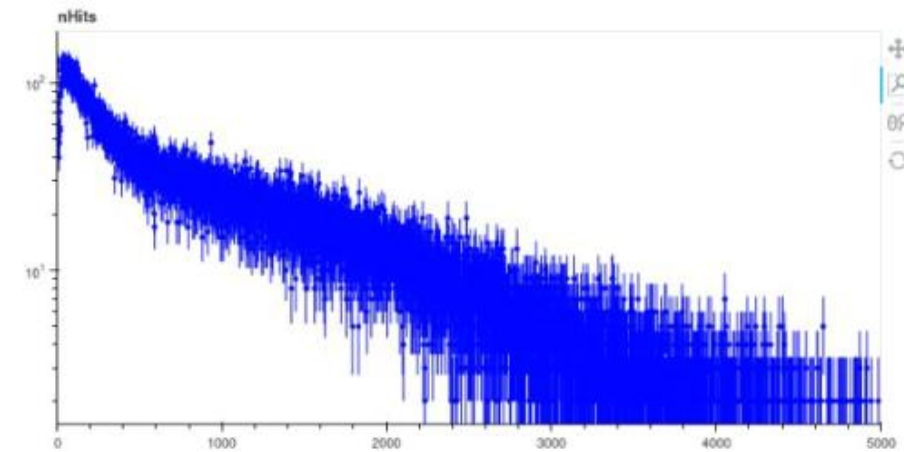
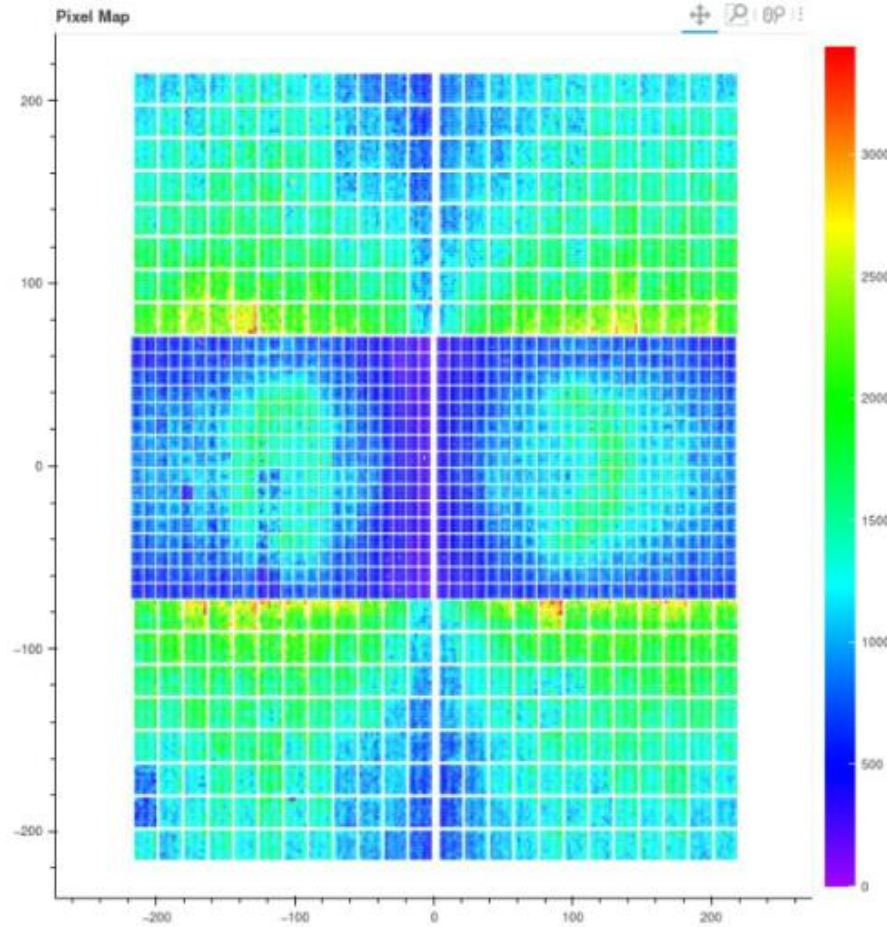


Collisions and Light (June-July 2022)

LHCb

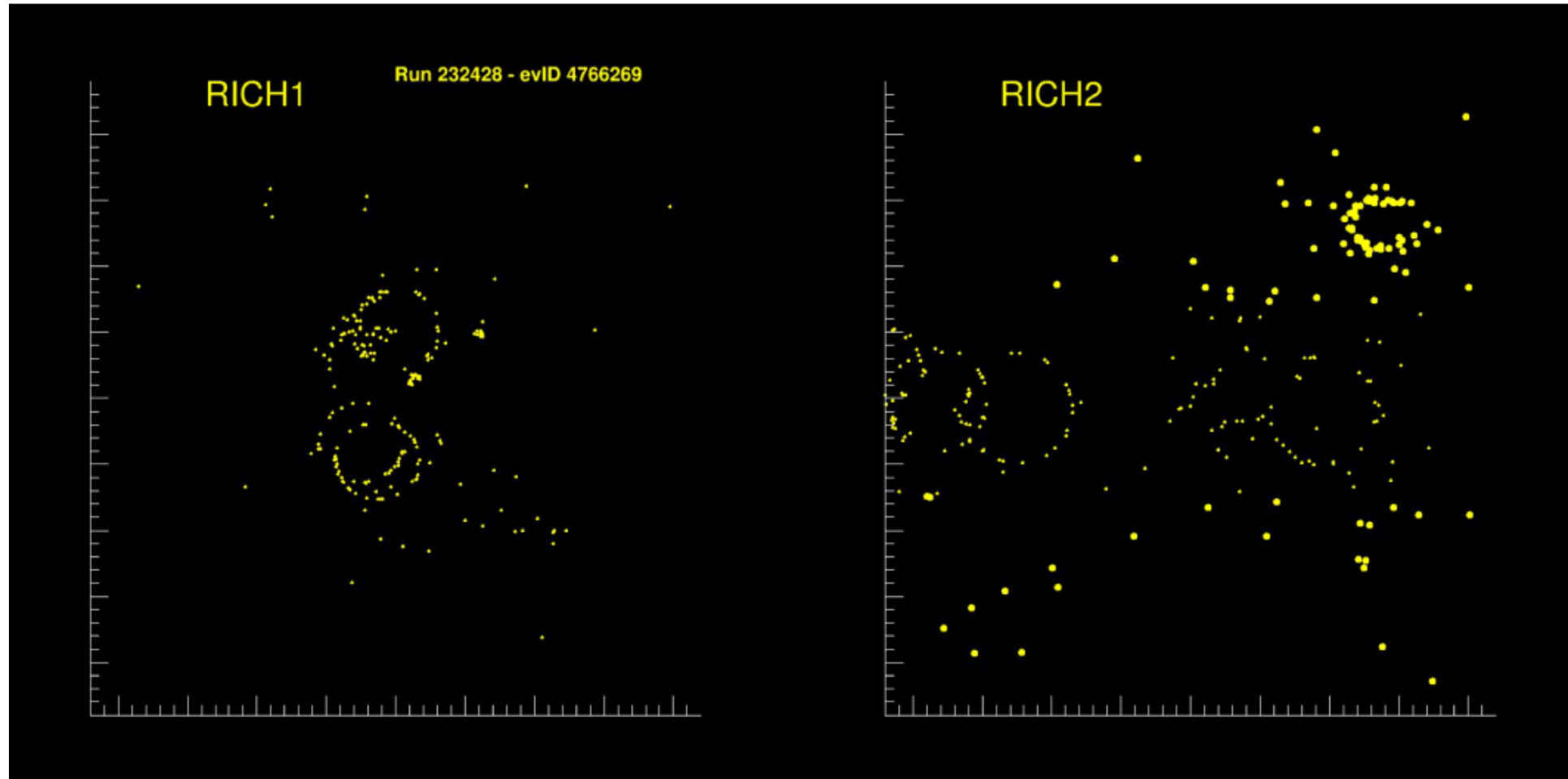
OnlineMon/RICH/RICH2

Save Rendering Info



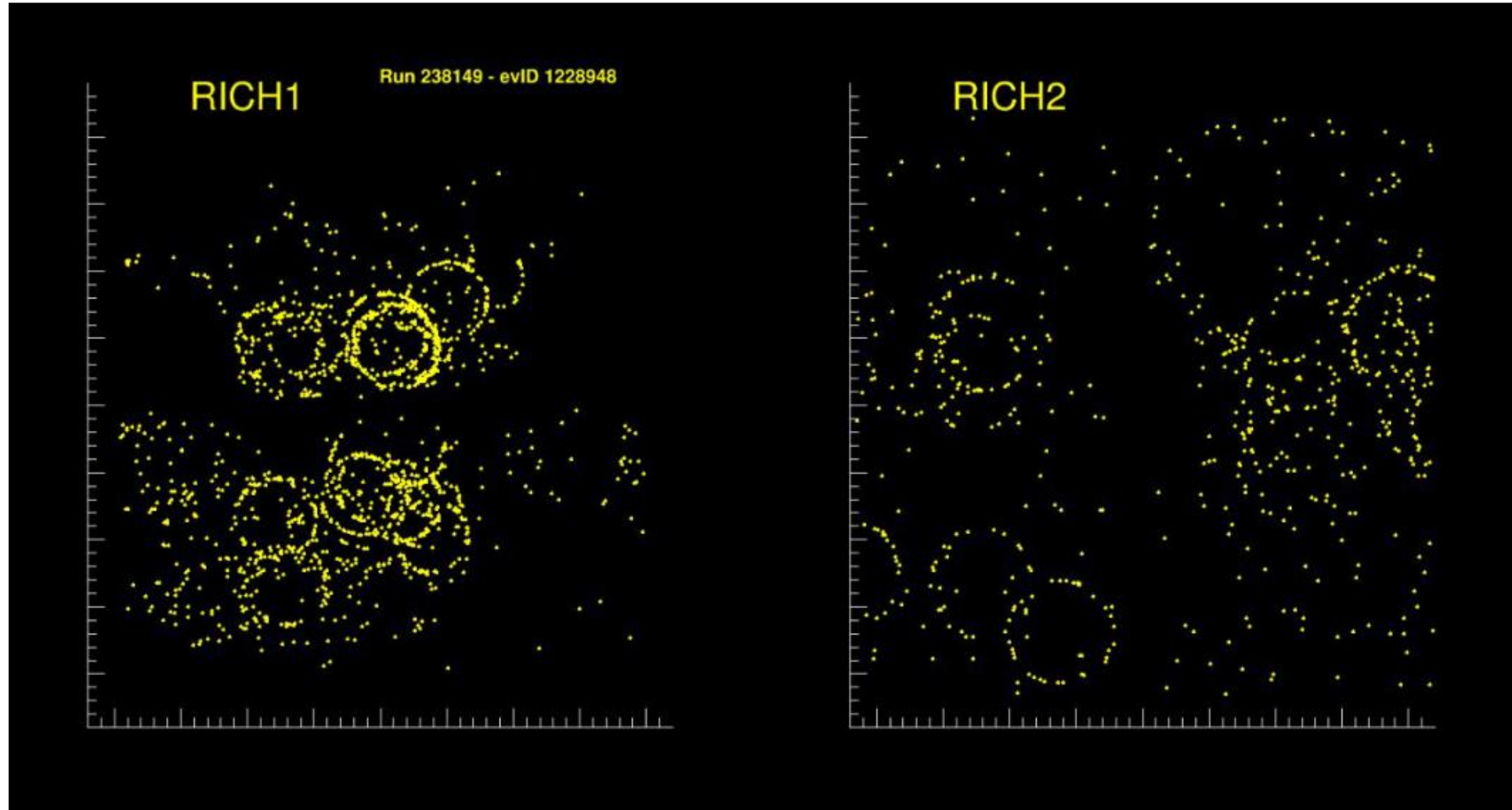
Collisions and Light (June-July 2022)

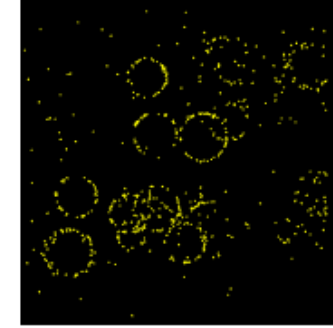
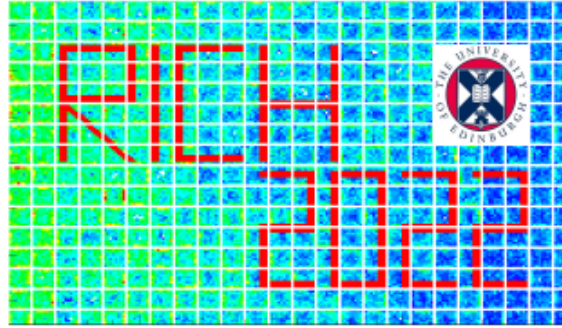
LHCb



Collisions and Light (June-July 2022)

LHCb





Characterisation and operations of the Multianode Photomultiplier Tubes for the LHCb RICH detectors

Giovanni Cavallero

CERN and Imperial College London

on behalf of the LHCb RICH collaboration

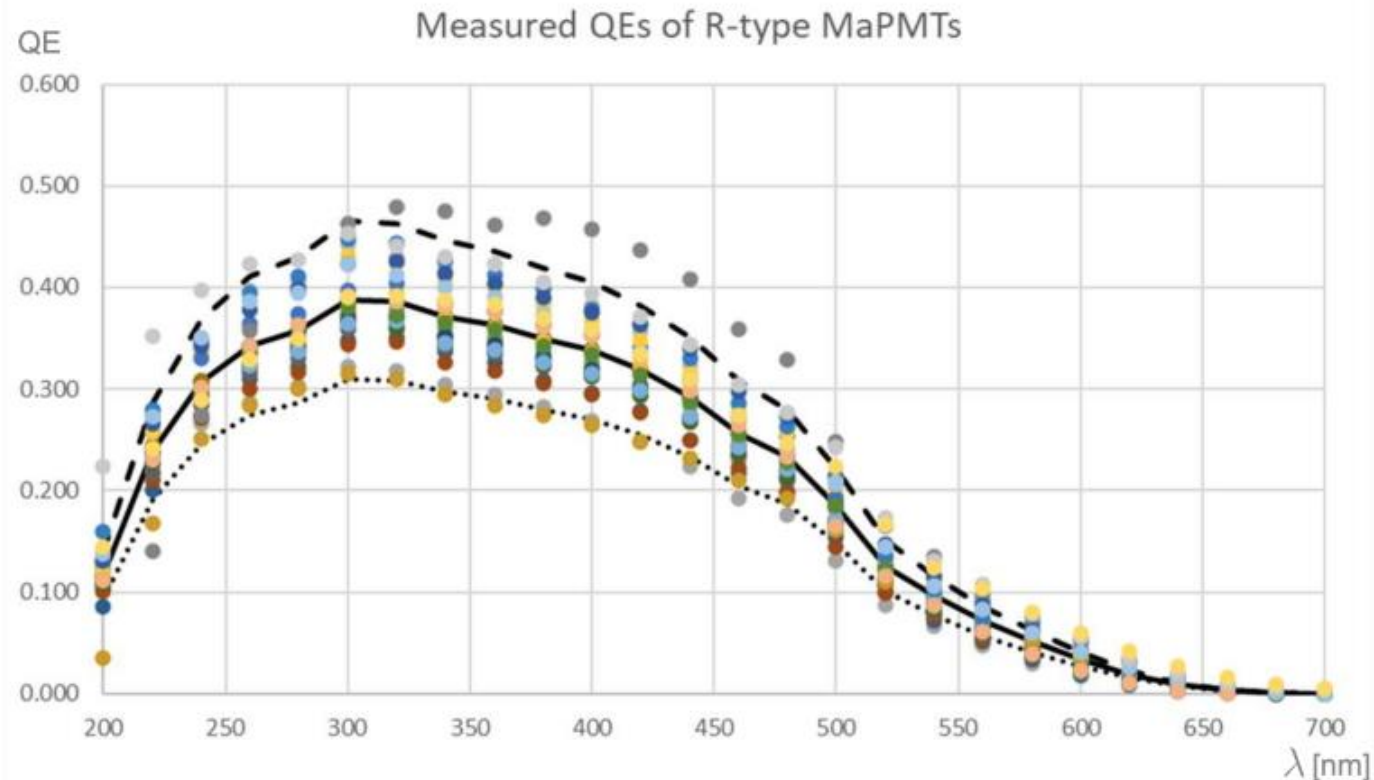
Imperial College
London



**RICH 2022,
12-16 September, Edinburgh, UK**

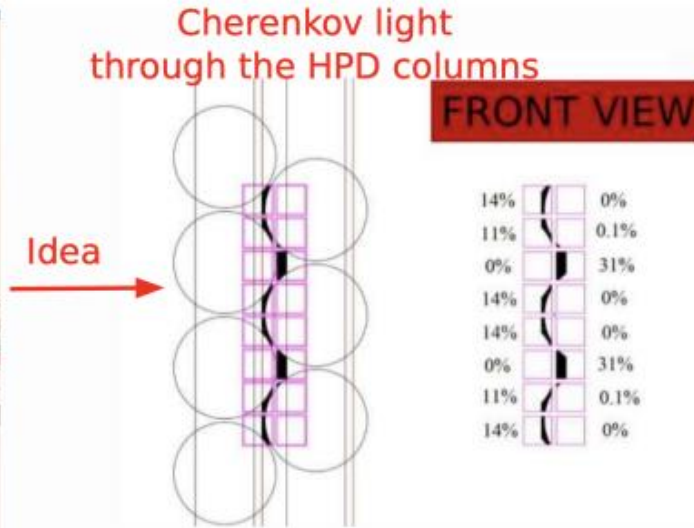
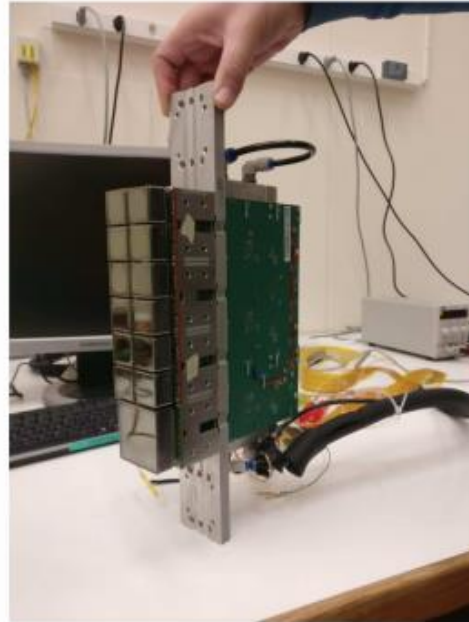
Quantum efficiency

- quantum efficiency measured in a dedicated setup at CERN on a subsample of devices (technical specification from Hamamatsu on the Blue Sensitivity Index)
- UV-glass entrance window: sensitivity to single-photon between 200 and 600 nm
- **ultra bi-alkali photocathodes allow to reach an excellent quantum efficiency of 40% at 300 nm in average!**



MaPMTs in the LHCb experiment during 2018 operations

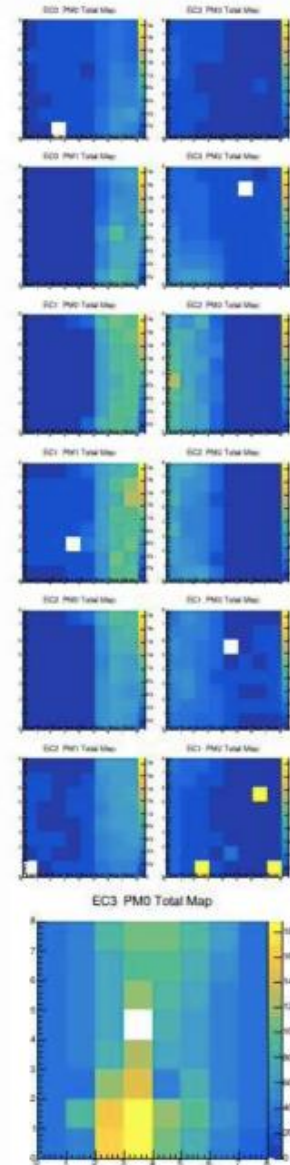
Aim: test a photon detection module in a realistic environment



Installation



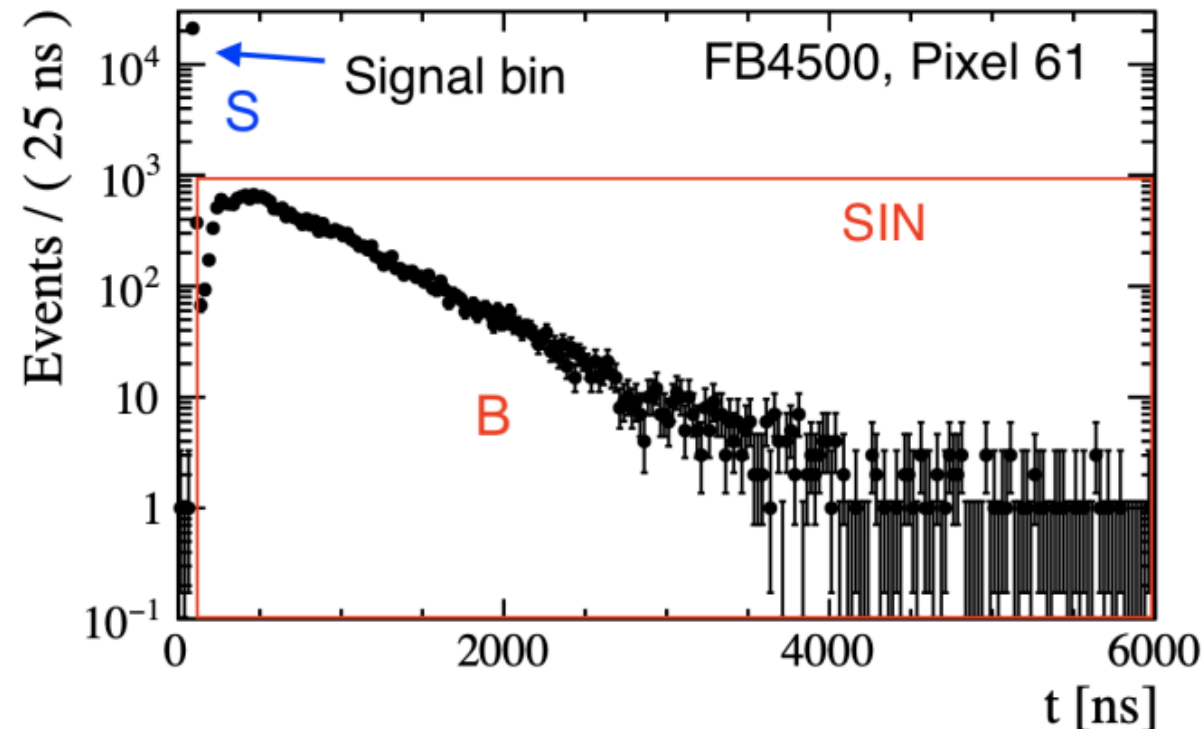
First collisions



Observation of Signal Induced Noise (SIN)

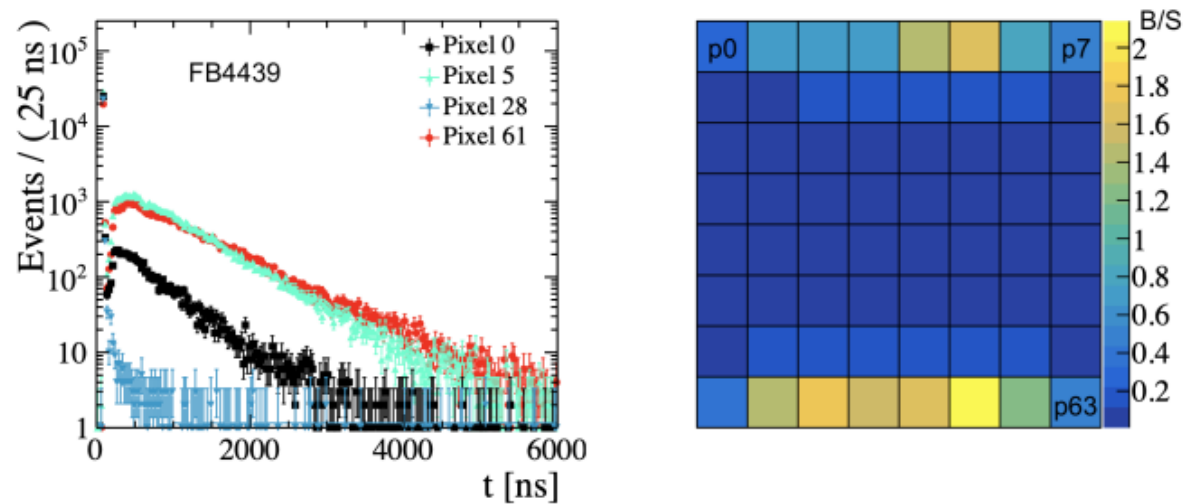
JINST 16 (2021) P11030

- first data acquired in an LHC collision scheme with isolated bunches (to synchronise the system) and with a $3 \mu\text{s}$ -wide acquisition window
- detection of **out-of-time hits** in R11265 tubes, delayed with respect to the expected arrival time of Cherenkov photons, indicating an unexpected source of noise
- characterised by the mean number of SIN pulses $\mu_{\text{SIN}} = B/S$



Localisation of SIN and device dependence

JINST 16 (2021) P11030



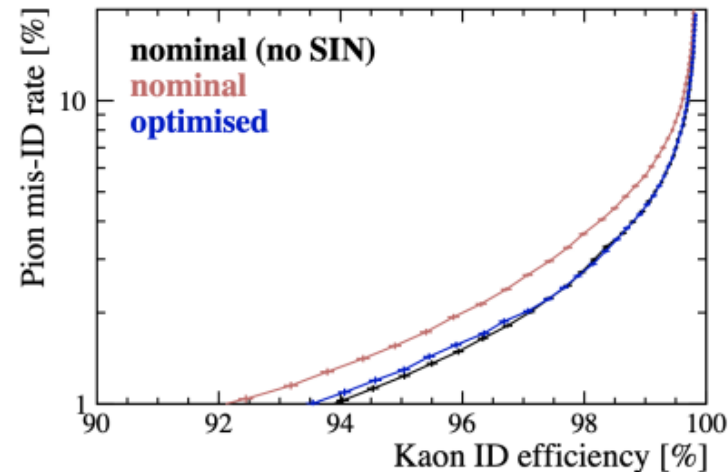
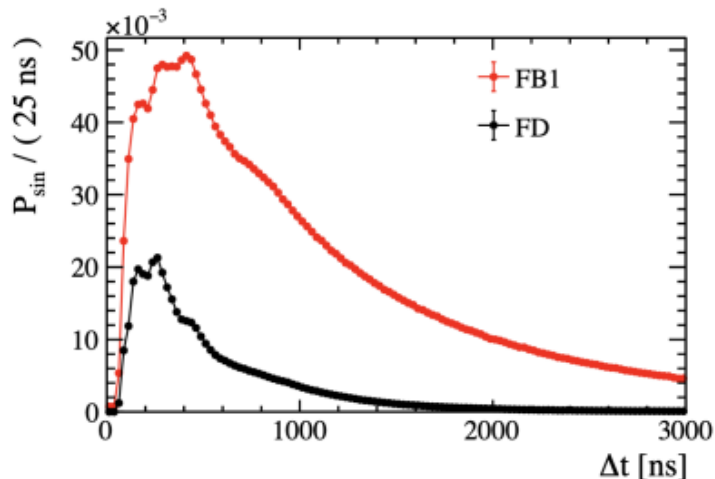
MaPMT	μ_{sin}^0	μ_{sin}^5	μ_{sin}^{28}	μ_{sin}^{61}
FB4439	0.2457 ± 0.0035	1.695 ± 0.013	0.0109 ± 0.0007	2.139 ± 0.018
FB2294	0.0745 ± 0.0012	0.3715 ± 0.0029	0.0076 ± 0.0004	0.491 ± 0.003
FB2312	0.132 ± 0.0017	0.747 ± 0.004	0.0081 ± 0.0004	2.231 ± 0.011
FB4500	0.266 ± 0.004	1.398 ± 0.012	0.0103 ± 0.0007	1.034 ± 0.010

- the localisation is a **general feature of SIN**, but with **absolute values of μ_{SIN} strongly depending on the device under consideration**
- weak correlation against the pixel gain, increasing at lower high-voltages
- no correlation with other MaPMT properties
- no connection between ageing effects and SIN and no significant changes when testing different voltage dividers

Mitigation strategies

JINST 16 (2021) P11030

- a **new series (FD)** of R11265 MaPMTs has been produced in 2019 by Hamamatsu to reduce the contributions of SIN pulses by means of a change of the internal mechanical design of the tube \Rightarrow installed in the central region of RICH1
- exploit the strong dependence on the HV to operate at the **lowest possible HV** as a compromise between single-photon detection efficiency and low SIN rate
- exploit the prompt (time spread: $\mathcal{O}(10 \text{ or } 100 \text{ ps})$) arrival time of Cherenkov photons on the photon detector planes to implement of a **6.25 ns time gate at the frontend readout** to increase the signal to noise ratio of a factor four (see **Floris Keizer's talk**)





A novel fast-timing readout chain for LHCb RICH LS3 enhancements and prototype beam tests

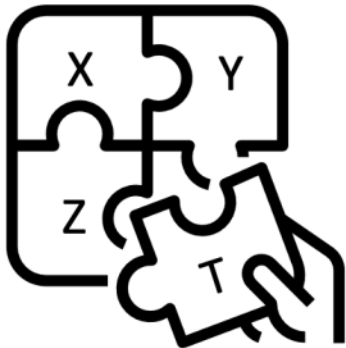
Floris Keizer on behalf of the LHCb RICH collaboration



11th International workshop on Ring Imaging Cherenkov Detectors,
RICH 2022, 12–16 September, Edinburgh

A time-resolved RICH detector

Promptly emitted Cherenkov photons + focusing mirror geometry
= For each track the signal arrives ~ simultaneously



In this presentation, aim to address:

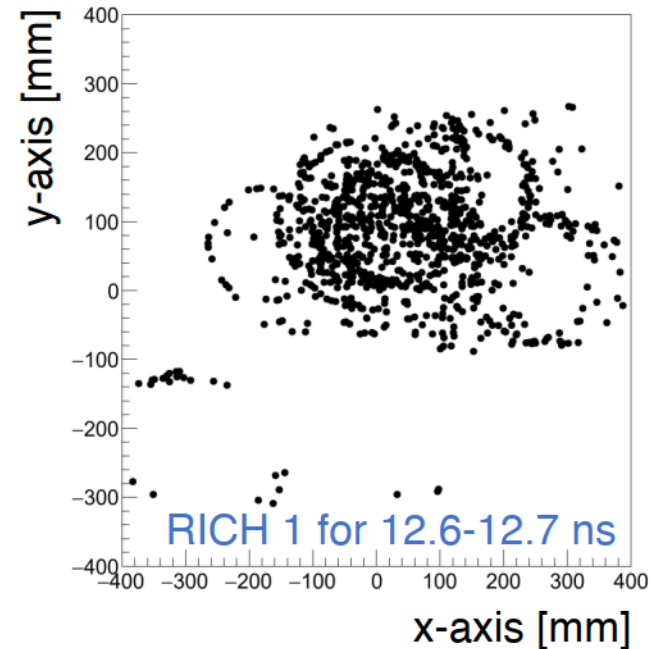
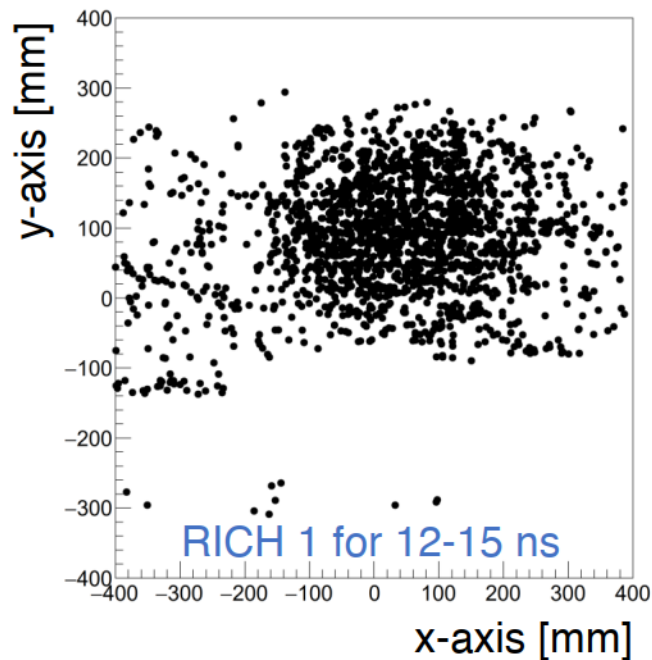
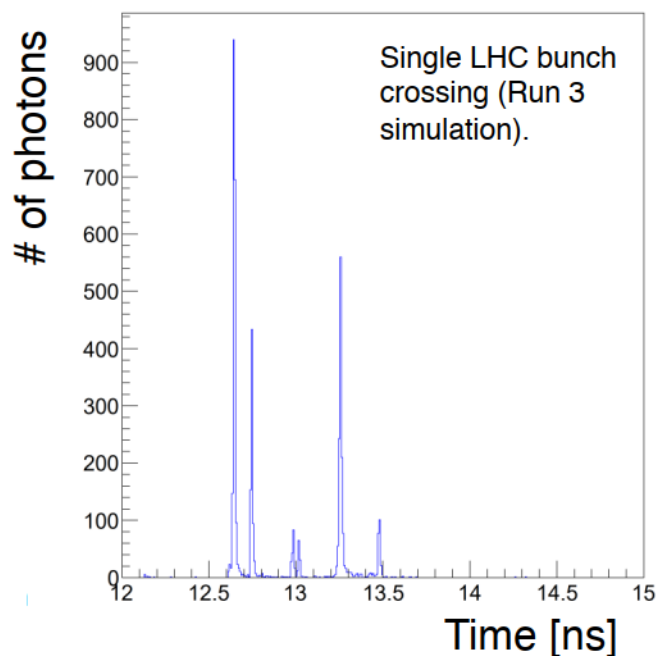
- **How** to make use of this feature to improve the PID.
- **Which** readout technologies and functionality to install during LHC Long Shutdown 3.
- **Prototype** developments and the ongoing test beam campaign.

Hit map for a single LHC bunch crossing (Run 3 simulation)

Simulating the Run 3 detector with an ‘ideal’ photon detector with zero time jitter shows distinct peaks originating from different Primary Vertices (PVs).

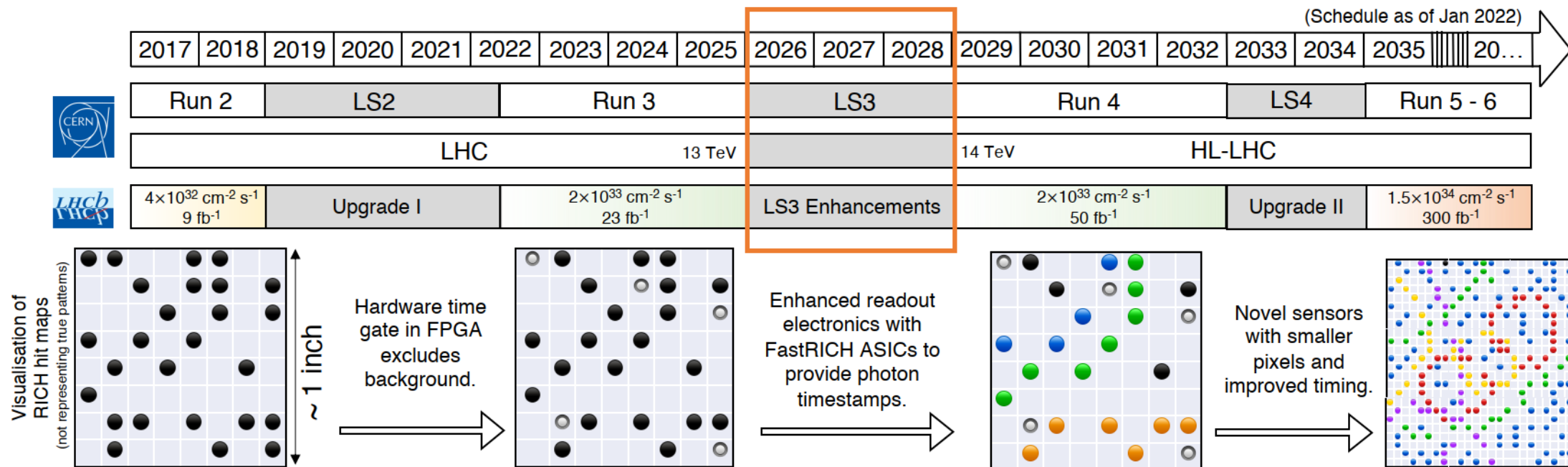
- In practice, the photon detector time **resolution blurs** the image in time.
- The RICH reconstruction maximum-likelihood approach works with **tracks and single hits**.

To reduce background and improve PID, need to accurately predict **when** the photons from a given track ought to arrive.



Evolution of the RICH photon detector

Relatively long period of LS3 central to the RICH evolution.

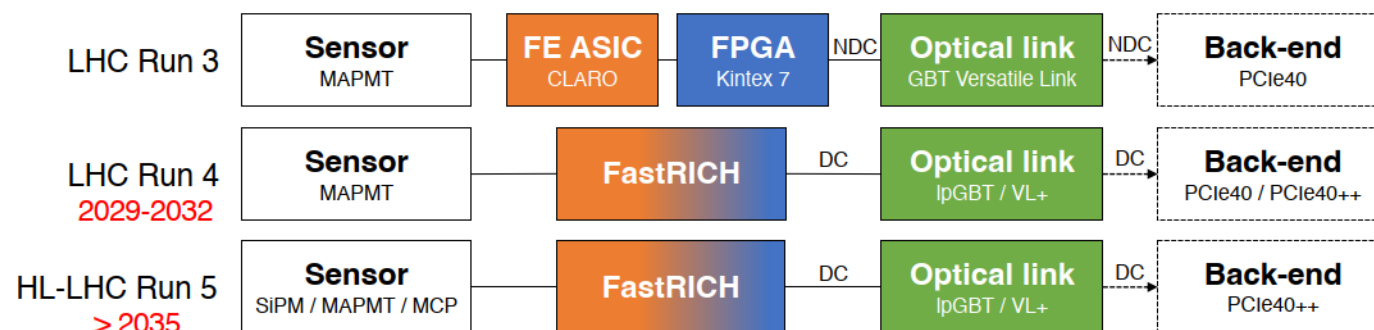


- LS3 / Run 4 : focus on **FastRICH** readout electronics with fast timing and wide input dynamic range.
- LS4 / Run 5 : focus on **sensor technology**. Fast-timing is essential for the luminosity challenge after Upgrade II. [[Talk](#) by Stephen Wotton]

Readout chain for LS3 and LS4

The LHCb RICH LS3 enhancements aim to equip the detector with new front-end readout electronics including the **FastRICH ASIC** capable of timestamping photon detector hits with ~ 25 ps time bins.

- ✓ Improve **PID performance during Run 4**.
- ✓ Introduce technologies for high-luminosity operation **ahead of Upgrade II**.
- ✓ Gather valuable experience with novel fast-timing and data compression techniques.



LS3 enhancements:

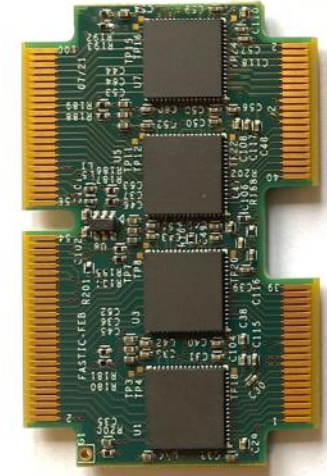
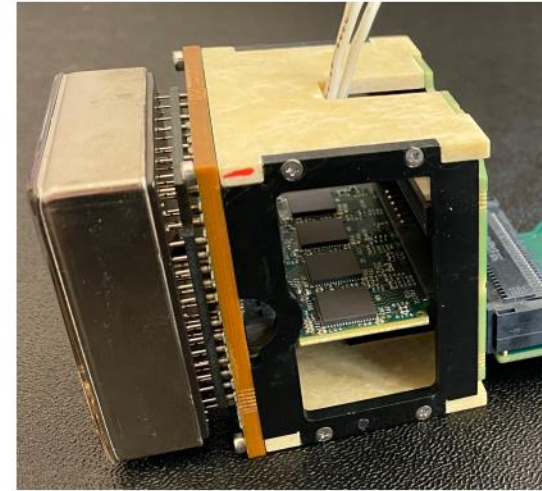
- Introduce FastRICH with 25 ps bins.
- Change to Data Compressed (DC) format.
- Introduce lpGBT/VL+.
- Small expansion at the back-end.

	Sensor	ASIC timewalk	FE time gate	TDC time bin
LHC Run 3	150 ps	< 4 ns	6.25 ns	None
LHC Run 4	150 ps	CFD correction	2 ns	25 ps
HL-LHC Run 5	~ 50 ps	CFD correction	2 ns	25 ps

FastIC and FastRICH ASICs [Poster by Rafael Ballabriga et al].

The Fast Integrated Circuit (**FastIC**) is an ASIC designed in 65 nm CMOS technology by the University of Barcelona (ICCUB) and CERN-EP-ESE.

- 8-channel chip with **wide input dynamic range** (5 μ A to 25 mA) for pos/neg signal polarities.
- **'Analog' ASIC** with fast discriminator (~ 30 ps jitter).
- **Not** designed to be specifically **radiation hard**.



RICH elementary cell with FastIC ASICs.

Next-generation **FastRICH** is based on the FastIC and **specific requirements of the RICH detector**.

- 16-channel chip with **analog and digital** signal processing.
- **Hardware shutter time** (configurable) to limit the timestamp range to ~ 1 to 2 ns.
- **Constant-fraction discrimination** (CFD).
- **Zero-suppressed** output over configurable number of output links to IpGBT.
- TDC with ~ 25 ps time bins and 40 MHz readout rate.
- Radiation hard by design ($\sim 10^{13}$ n_{eq}/cm^2 and ~ 5 kGy).
- Compatibility with IpGBT and the architecture of the Run 4 and Run 5 DAQ.

FastRICH design is ongoing (CERN-ICCUB) with the analog parts far advanced.

The prototype fast-timing readout chain

Digital board for the testbeam, containing a Kintex7
FPGA with 34-channel TDC with 150 ps time bins

➤ [[Poster](#) by Lucian Cojocariu et al].

FEBs with **FastIC** ASICs.

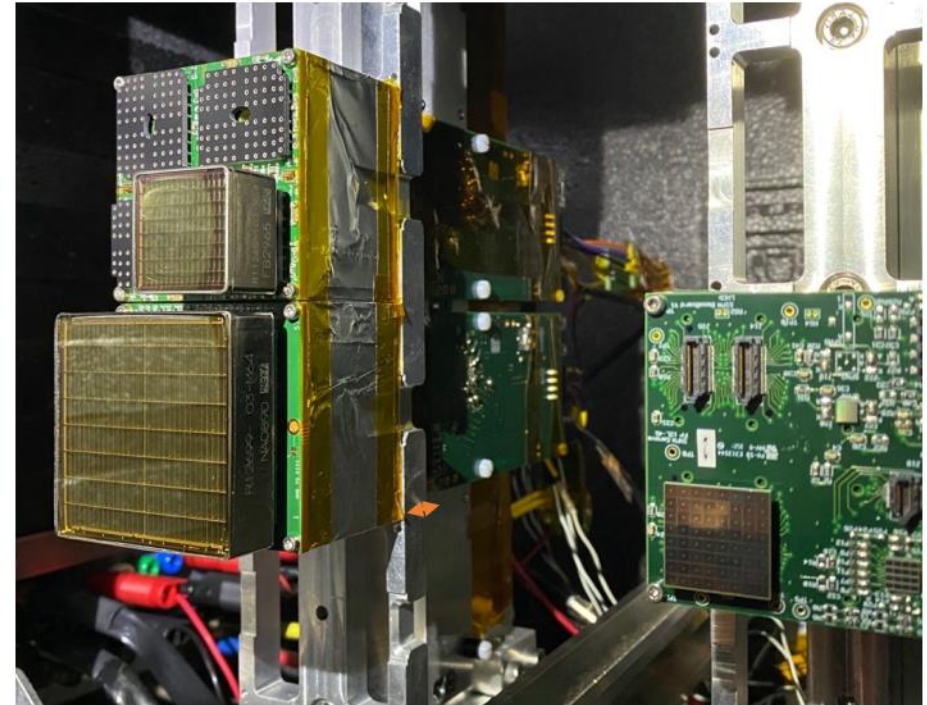
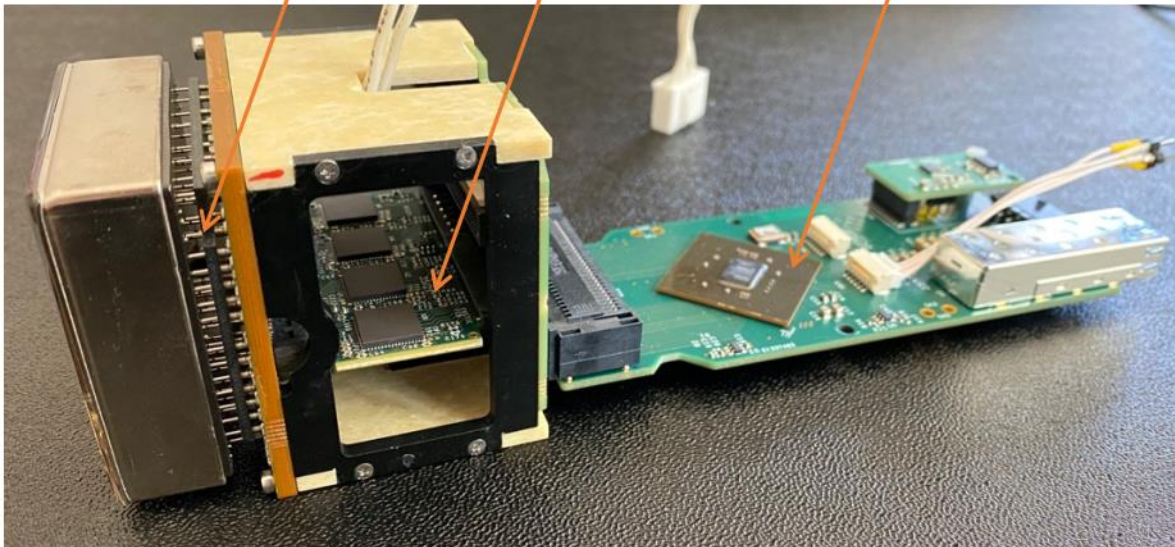
➤ Output of fast-timing channel:
ToA + **non-linear ToT**.

MAPMT / SiPM baseboard.

➤ [[Talk](#) by Roberta Cardinale]

FastICs **coupled to MAPMTs**
(1 and 2-inch devices, Run 4)

and an **SiPM array** (Run 5 candidate).



LHCb RICH Upgrade II

XI International Workshop on Ring Imaging Cherenkov Detectors,
RICH 2022, 12th-16th September



Steve Wotton
University of Cambridge

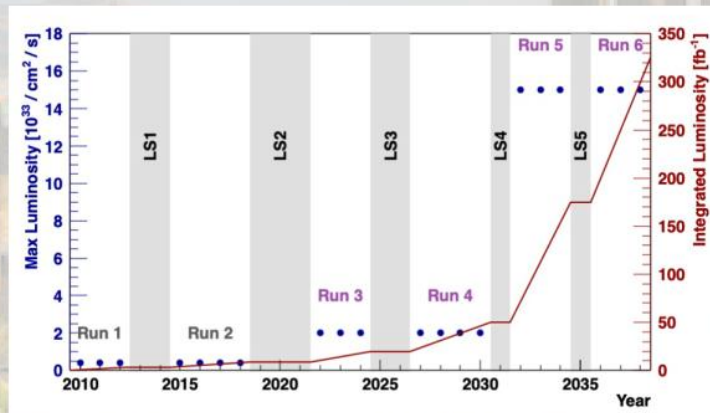
on behalf of the LHCb RICH collaboration



LHCb & the High Luminosity LHC

From around 2035 the LHCb physics program will benefit from a factor 7.5 increased luminosity compared to Run 4. The full Upgrade program is described in the recently published FTDR.

The RICH detectors will remain a vital element of LHCb and will be essential to exploit new physics opportunities in this new high luminosity era (Run 5 & Run 6).



Luminosity: $1.5 \times 10^{34} \text{ cm}^{-2} \text{ s}^{-1}$
RICH1 n-equivalent dose: $\sim 10^{13} \text{ cm}^{-2}$ (1 MeV equivalent)
Total Ionising Dose: $\sim 5 \text{ kGy}$ for 350 fb^{-1}



<https://cdsweb.cern.ch/record/2776420/>

Chromatic Error

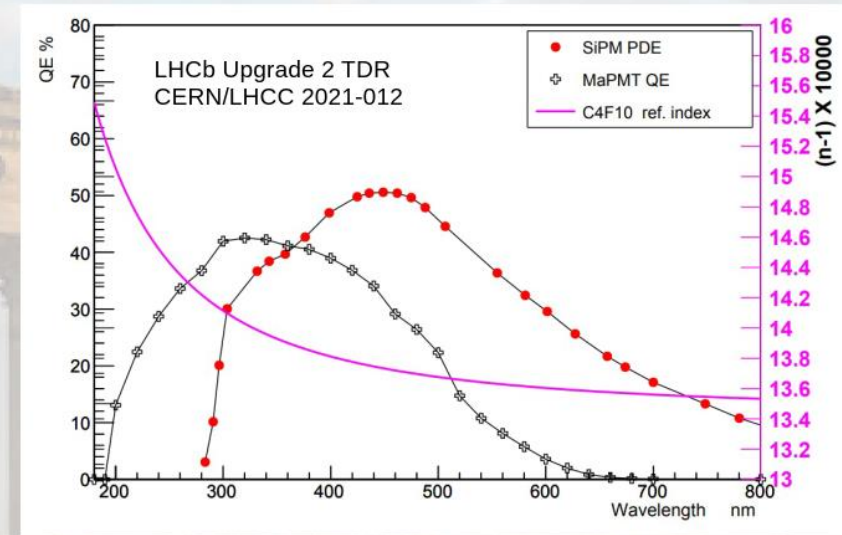
The wavelength dependence of the refractive index gives rise to a chromatic error that can be a significant contribution to the overall error.

This chromatic error is driven by the convolution of:

- Cherenkov photon spectrum;
- spectral sensitivity of the sensor;
- absorption coefficients;
- reflectivity.

There is a clear benefit to operating at longer wavelength where the photon spectrum is flatter.

For example, by using SiPMs as the photon sensor and with optimisation of the optical layout, we estimate a contribution of about 0.1 mrad.



	Current	Future
RICH1 [mrad]	0.52	0.11
RICH2 [mrad]	0.34	0.10

Emission Point Error

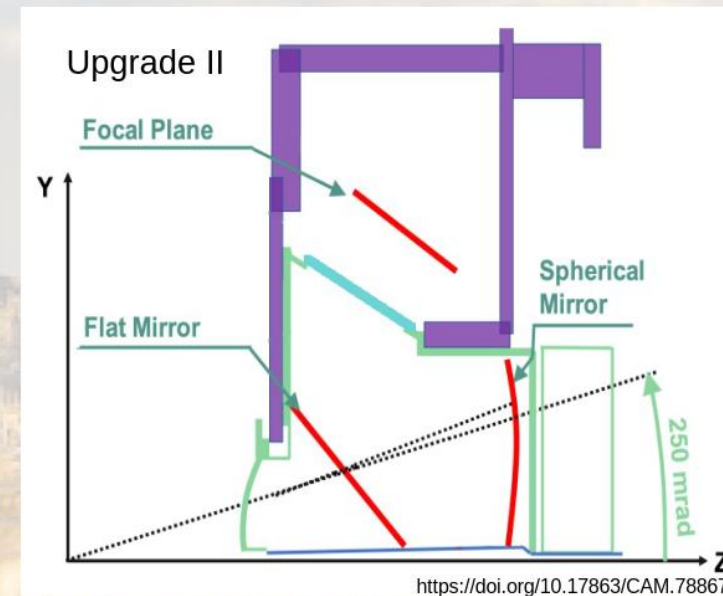
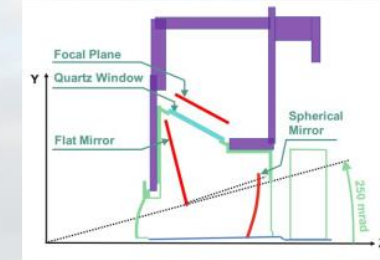
In LHCb, the spherical mirror is tilted to allow the sensor region to be kept outside the detector acceptance.

This introduces an error that arises from optical aberrations that make the detected photon position depend on its emission point within the radiator volume.

Closer to ideal geometry can be achieved with smaller mirror tilt:

- Flat mirrors move inside the acceptance
- Must be made of light materials

By making this change we estimate that the emission point error can be reduced to 0.12mrad



	Current	Future
RICH1 [mrad]	0.36	0.12
RICH2 [mrad]	0.32	0.05

Summary of contributions to angular resolution

Configuration	Overall [mrad]	Chromatic [mrad]	Emission pt [mrad]	Pixel [mrad]	Yield
RICH 1					
MaPMT	0.8	0.52	0.36	0.5	63
SiPM	0.40	0.11	0.36	0.15	47
SiPM+geom	0.22	0.11	0.12	0.15	34
RICH2					
MaPMT	0.50	0.34	0.32	0.22	34
SiPM+geom	0.13	0.10	0.05	0.07	20-30

Significant improvements are possible with respect to the current LHCb RICH configuration.

The table compares expectations for the current MaPMT RICH with a possible future design using SiPMs

Realising these improvements also requires corresponding improvements in tracking performance.

The impact on PID performance

The better the photon time resolution the better the PID performance.

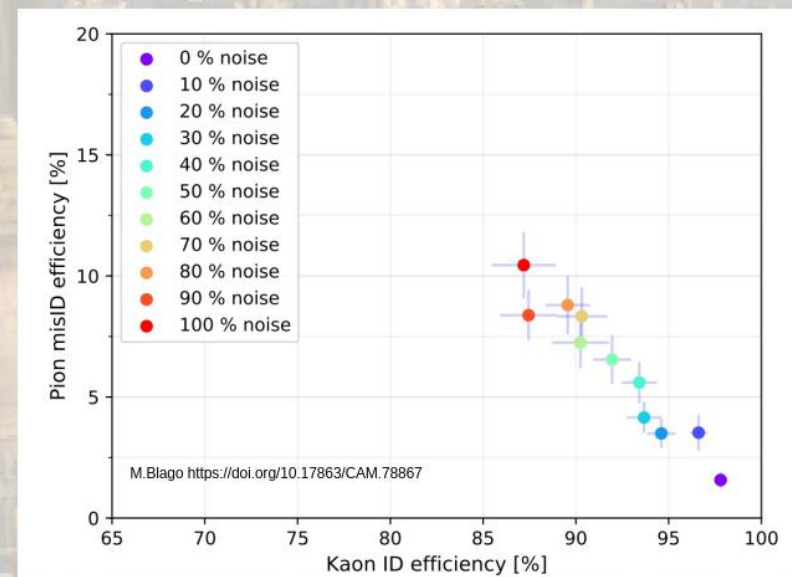
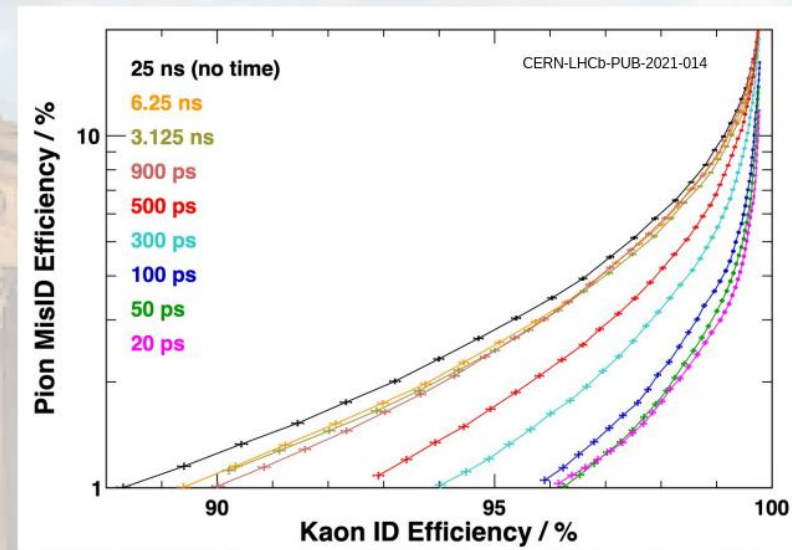
The curves in upper plot are a standard metric that we use in LHCb to characterise PID performance.

Best performance is furthest to the right and bottom.

i.e. High Kaon efficiency with low Pion misidentification probability

Effect seen in both conventional (global maximum likelihood) reconstruction and when using CNNs (lower plot).

The benefit arises because better timing allows tighter cuts to remove out-of-time photons.



Summary of Sensor Attributes

	MaPMT	SiPM	MCP/LAPPD
σ_t [ps]	150	60	30
Pixel size [mm]	≥ 2.8	≥ 1	Custom (R&D)
QE	> 35% at 350 nm	> 45% at 460 nm	20-30% at 350 nm
Dark count rate [Hz mm ⁻²]	1	$10^5 - 10^7$	1
Typical operating voltage	1 kV	< 100 V	1 kV
B-field	< 5 mT	Insensitive	< 2 T
Radiation tolerance	Entrance window	Lattice defects	Entrance window
Gain ageing limits	$I_{\text{anode}} 100 \mu\text{A}$	N/A	10 C cm^{-2}

There is not yet a candidate sensor that is proven to meet all LHCb Upgrade 2 requirements but there are candidates that come very close.

Further R&D is needed.



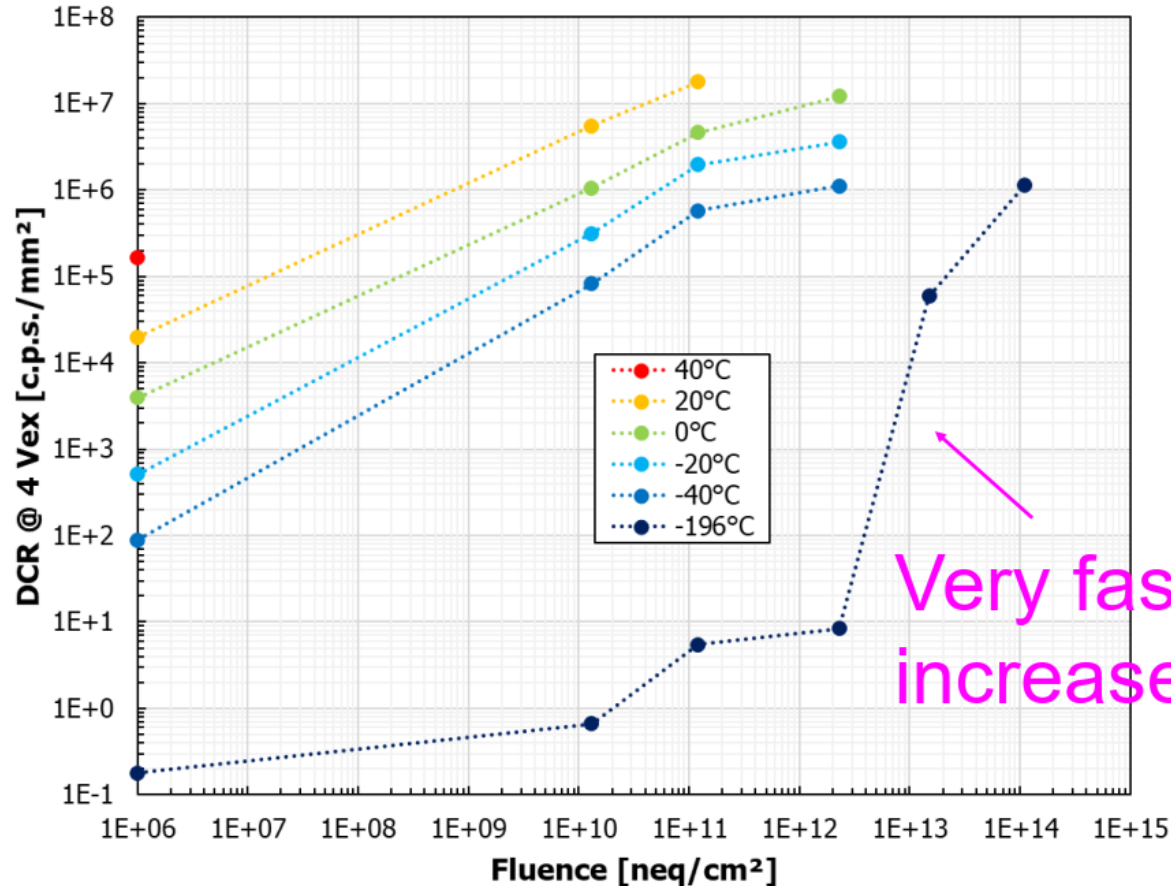
Status and perspectives of SiPMs

Alberto Gola
Chief Scientist

F. Acerbi, A. Ficorella, S. Merzi, L.P. Monreal, E. Moretti, G.
Paternoster, M. Penna, M. Ruzzarin, N. Zorzi

Test Beam 2 – LNS Catania

DCR at LN after irradiation



- Cooling is *extremely effective in reducing DCR after irradiation up to $\sim 1 \cdot 10^{12} n_{eq}/cm^2$*
- Further investigations needed to understand what happens at the higher doses
- Worth checking different / new SiPM structures
- Check possible effect of annealing

Radiation Hardness

Definition + Mitigation strategies

It is rather obvious that *we cannot prevent the bulk damage from increasing the DCR* of the SiPM.

A *possible definition of Rad-Hardened / tolerant SiPM* is a *SiPM that retains its target performance in a given application* even after radiation damage.

→ Depends on the application!

→ *Radiation damage mitigation strategies* (+ annealing)

Use of small cells + Engineering of electric field

Issue / Hypothesis	Technical Solution	Mitigation
Increase of primary DCR	Electric field engineering	Better DCR temperature coefficient High PDE at lower bias (to reduce field-enhanced effects)
PDE loss due to cells busy triggering dark counts.	Smaller Cells	More cells and faster recharge: lower PDE loss.
Increased power consumption due to higher DCR.	Smaller Cells	Lower gain: less current (for a given DCR).



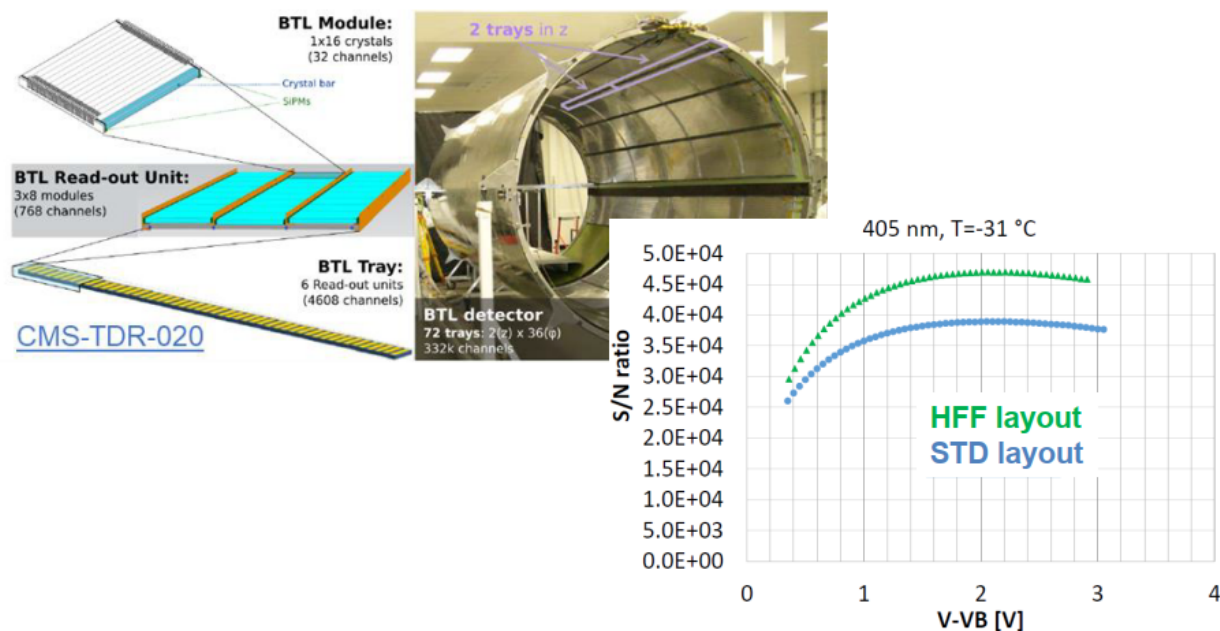
.. But, at the same time, we need high PDE!

Mitigation of Radiation Damage

NUV-HD-RH SiPMs for CMS-BTL

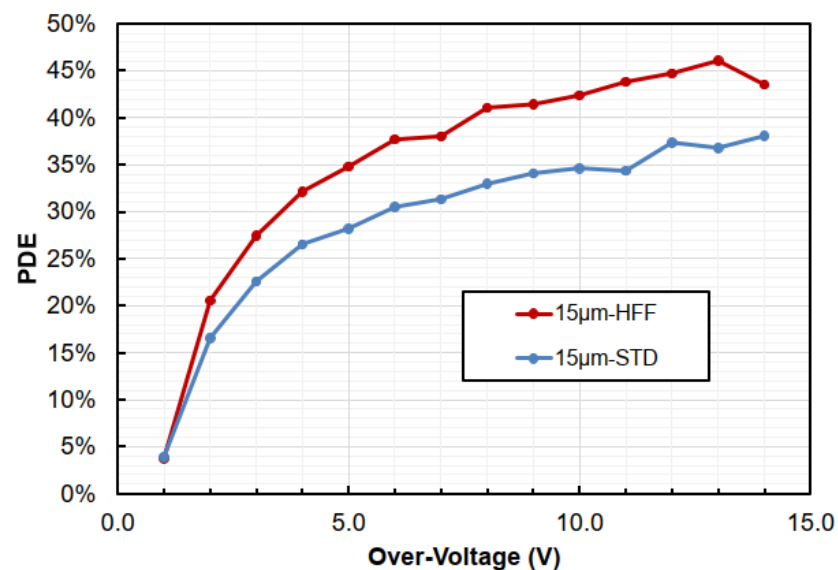
SiPMs with extreme radiation tolerance are required for the Barrel Timing Layer of the CMS experiment, at CERN: $1.9 \times 10^{14} \text{ 1 MeV } n_{\text{eq}}/\text{cm}^2$.

Custom SiPM technology was developed, combining *electric field engineering with small-pitch SiPM technology*, for enhanced radiation hardness.



FoM measured by from CMS collaboration:
A. Heering, Y. Musienko, M. Lucchini et al.)

NUV-HD-RH SiPMs



The advantage of using small cells for radiation hardness is relevant *only if they can still provide very high PDE*